



1 **Sources and Transformations of Anthropogenic Nitrogen along an Urban River-**  
2 **Estuarine Continuum**

3

4 Michael J. Pennino\*<sup>1</sup>, Sujay S. Kaushal<sup>2</sup>, Sudhir Murthy<sup>3</sup>, Joel Blomquist<sup>4</sup>, Jeff  
5 Cornwell<sup>5</sup>, and Lora Harris<sup>6</sup>

6

7 <sup>1</sup>Department of Civil and Environmental Engineering, Princeton University, Princeton,  
8 NJ, USA.

9 <sup>2</sup>Department of Geology and Earth Systems Science Interdisciplinary Center, University  
10 of Maryland, College Park, MD, USA.

11 <sup>3</sup>DC Water, Washington, DC, USA.

12 <sup>4</sup>U.S. Geological Survey, Baltimore MD, USA.

13 <sup>5</sup>Center for Environmental Science, University of Maryland Horn Point Laboratory,  
14 Cambridge, MD, USA.

15 <sup>6</sup>Center for Environmental Science, University of Maryland Chesapeake Biological  
16 Laboratory, Solomons MD, USA.

17 \*Corresponding author email: Michael.pennino@gmail.com

18

19

20

21

22

23



24 **Abstract**

25 Urbanization has altered the fate and transport of anthropogenic nitrogen (N) in rivers  
26 and estuaries globally. This study evaluates the capacity of an urbanizing river-estuarine  
27 continuum to transform N inputs from the world's largest advanced (e.g. phosphorus and  
28 biological N removal) wastewater treatment facility. Effluent samples and surface water  
29 were collected monthly along the Potomac River Estuary from Washington D.C. to the  
30 Chesapeake Bay over 150 km. In conjunction with box model mass balances, nitrate  
31 stable isotopes and mixing models were used to trace the fate of urban wastewater nitrate.  
32 Nitrate concentrations and  $\delta^{15}\text{N-NO}_3^-$  values were higher down-estuary from the Blue  
33 Plains wastewater outfall in Washington D.C. ( $2.25\pm 0.62$  mg/l and  $25.7\pm 2.9\%$ ,  
34 respectively) compared to upper-estuary concentrations ( $1.0\pm 0.2$  mg/l and  $9.3\pm 1.4\%$ ,  
35 respectively). Nitrate concentration then decreased rapidly within 30 km down-estuary  
36 (to  $0.8\pm 0.2$  mg/l) corresponding with an increase in organic nitrogen and dissolved  
37 organic carbon, suggesting biotic uptake and organic transformation. TN loads declined  
38 down-estuary (from an annual average of  $48,000\pm 5,000$  kg/day at the sewage treatment  
39 plant outfall to  $23,000\pm 13,000$  kg/day at the estuary mouth), with the greatest percentage  
40 decrease during summer and fall. 4–71% of urban wastewater TN inputs were exported  
41 to the Chesapeake Bay, with the greatest contribution of wastewater TN loads during the  
42 spring. Our results suggest that biological transformations along the urban river-estuary  
43 continuum can significantly transform wastewater N inputs from major cities globally,  
44 but more work is necessary to evaluate the potential of organic nitrogen to contribute to  
45 eutrophication and hypoxia.

46



47 **Key Words**

48 Estuary, Mass Balance, Mixing Model, Nitrate Isotopes, Source Tracking, Wastewater

49 **1 Introduction**

50 Urbanization and agriculture have greatly increased the exports of nitrogen from  
51 coastal rivers and estuaries globally, contributing to eutrophication, hypoxia, harmful  
52 algal blooms, and fish kills (e.g. Aitkenhead-Peterson et al., 2009; Kaushal et al., 2014b;  
53 Nixon et al., 1996; Petrone, 2010; Vitousek et al., 1997). Despite billions of dollars spent  
54 on regulatory and technological improvements for wastewater treatment plants (WWTPs)  
55 and agricultural and urban stormwater runoff (e.g. US-EPA, 1972, 2009, 2011), many  
56 coastal waters are still impaired. Also, there are major questions regarding how far urban  
57 sources of N (wastewater and stormwater runoff) are transmitted along tidal river-  
58 estuarine networks to N-sensitive coastal receiving waters. This study evaluates the  
59 capacity of a major river-estuarine system to transform and attenuate N inputs from the  
60 world's largest advanced (e.g. phosphorus and biological nitrogen removal) wastewater  
61 treatment plant (Blue Plains) before being transported down-estuary to the Chesapeake  
62 Bay. We used a combination of stable isotope and box model mass balance approaches  
63 to track the fate and transport of anthropogenic nitrogen across space and time.

64 In addition to urban and agricultural inputs, altered river-estuarine hydrology can  
65 contribute to higher exports of N. Jordan et al. (2003) found that annual water discharge  
66 increased as the proportion of developed land in a coastal watershed increased. Higher  
67 flows, typically during winter and spring months, have also been associated with higher  
68 N loads in coastal river-estuaries (Boynton et al., 2008). Furthermore, regional climate



69 variability amplifies pulses of nutrients and other contaminants in rivers (Easterling et al.,  
70 2000; IPCC, 2007; Kaushal et al., 2010b; Saunders and Lea, 2008) and alters the biotic  
71 transformation of N due to changes in hydrologic residence times (Hopkinson and  
72 Vallino, 1995; Kaushal et al., 2014b; Wiegert and Penaslado, 1995). For example, high  
73 flow periods related to storms can induce stratification and impact salinity regimes  
74 (Boesch et al., 2001), which affects nutrient biogeochemistry like ammonium and  
75 phosphate concentrations (Jordan et al., 2008). An improved understanding of the  
76 longitudinal assimilatory capacity for nitrogen by large river-estuarine systems across  
77 different flow regimes is needed for guiding effective coastal river and estuarine  
78 management strategies.

79         One critical and innovative approach to effectively manage coastal nutrient  
80 pollution is to 1) track the relative contributions of N export from different sources within  
81 the watershed and 2) understand the potential for longitudinal transformation within  
82 coastal rivers and estuaries. Recent studies using stable isotopes (Kaushal et al., 2011;  
83 Kendall et al., 2007; Oczkowski et al., 2008; Wankel et al., 2006) have shown that these  
84 methods can be helpful in elucidating sources and transformations of nitrogen. However,  
85 these studies are typically conducted at relatively smaller spatial scales and without  
86 coupling to mass balance approaches over both time and space.

87         Here, we combine isotope and mass balance approaches to track sources and  
88 transformations of urban wastewater inputs to Chesapeake Bay over space and time  
89 across an urban river-estuary continuum spanning over 150 km. The space-time  
90 continuum approach has previously been used in studying fate and transport of carbon  
91 and nitrogen in urban watersheds (Kaushal and Belt, 2012; Kaushal et al., 2014c), and



92 here we explore extending it to river and estuarine ecosystems. Our overarching  
93 questions were: 1) how does the importance of point vs. non-point sources of N shift  
94 along a tidal and stratified urban river-estuary continuum across space and time? 2) What  
95 is the capacity of an urban river-estuary continuum to transform or assimilate  
96 anthropogenic N inputs? 3) How are transport and transformations of N affected by  
97 differences in season or hydrology? An improved understanding of how sources and  
98 transformations of N change along the urban river-estuarine continuum over space and  
99 time can inform management decisions regarding N source reductions along urbanizing  
100 coastal watersheds (e.g. Boesch et al., 2001; Kaushal and Belt, 2012; Paerl et al., 2006).

## 101 **2 Methods**

### 102 **2.1 Site Description**

103 This study is focused on the tidal Potomac River Estuary, which includes the  
104 section of the river from Washington D.C. to its confluence with the Chesapeake Bay  
105 (Fig. 1). The Potomac River Estuary begins as tidal freshwater, becoming oligohaline  
106 ~30-50 km below Washington D.C., and mesohaline at its mouth approximately 160 km  
107 below Washington D.C. (Jaworski et al., 1992). The Potomac River Estuary can be  
108 seasonally stratified (Hamdan and Jonas, 2006), especially in the southern portion of the  
109 system where intruding, saline bottom water from the main stem of the Chesapeake Bay  
110 leads to density driven estuarine circulation patterns (Elliott, 1976, 1978; Pritchard,  
111 1956). Mixing is most evident at the estuarine turbidity maximum (Hamdan and Jonas,  
112 2006), ~60-80 km below Washington D.C., and the water column is generally well mixed  
113 above the estuarine turbidity maximum zone in the tidal fresh and oligohaline regions of



114 the estuary (Crump and Baross, 1996; Sanford et al., 2001).

115 The watershed draining to the Potomac River Estuary is classified as 58% forested,  
116 23% agricultural, and 17% urban, based on Maryland Department of Planning data for  
117 2002 (Karrh et al., 2007a). Based on the Chesapeake Bay Program (CBP) Model it was  
118 estimated that during 2005 total inputs of nitrogen were 33% from agriculture, 20% from  
119 urban (e.g. stormwater runoff and leaky sewers), 19% from point sources (wastewater  
120 treatment plants and industrial releases), 11% from forest, 10% from septic, 6% from  
121 mixed open land, and 1% from atmospheric deposition to water (Karrh et al., 2007b).

122 The CBP model is developed using long-term monitoring data and the non-point loads  
123 are estimated from a variety of sources including land cover and agriculture records  
124 (Karrh et al., 2007b). The Potomac River Estuary also receives N inputs from Blue  
125 Plains wastewater treatment plant, located in Washington, D.C. Blue Plains currently  
126 discharges 2.3 mg/L of  $\text{NO}_3^-$  and 3.7 mg/L of TN, on average, and exports loads of  
127 approximately 2,300 kg/day of  $\text{NO}_3^-$  and 3,900 kg of TN. Overall, Blue Plains treats and  
128 discharges 280 million gallons per day (mgd), almost 5% of Potomac River's annual  
129 discharge. In the past several decades, Blue Plains has undergone several technological  
130 improvements with phosphorus removal in the 1980s and enhanced N removal beginning  
131 in the year 2000. Since the implementation of advanced wastewater treatment  
132 technologies at Blue Plains, there has been a significant decrease ( $p < 0.01$ ) in the  
133 concentration of nitrate in effluent discharge, from an average of  $7.2 \pm 0.3$  mg/L before  
134 the year 2000 (years 1998 and 1999) to an average of  $4.1 \pm 0.4$  mg/L after 2000 (years  
135 2001 to 2008).

136



137 **2.2 Analysis of long-term spatial and temporal water chemistry data**

138 Surface and bottom water N and carbon data collected by the Maryland  
139 Department of Natural Resources (DNR) and accessed through the Chesapeake Bay  
140 Program's data hub website (Chesapeake Bay Program, 2013) was used to look at  
141 historical (1984 to 2012) monthly nutrient concentrations from stations located  
142 longitudinally along the Potomac River Estuary (Fig. 1). These data were used to look at  
143 the spatial and temporal trends for dissolved and particulate forms of N and dissolved  
144 organic carbon (DOC) in the Potomac River Estuary prior to and during this study.

145

146 **2.3 Water Sampling**

147 Water samples along the Potomac River estuary were collected monthly for one  
148 year from April 2010 to May 2011; from 12 km to 160 km below the Blue Plains  
149 wastewater treatment plant (See Fig. 1). Water was collected from the surface (top 0.5  
150 m) and bottom water depths. Additionally, surface water samplings from 6 km above to  
151 12 km below the Blue Plains wastewater treatment plant effluent outfall were collected  
152 seasonally during this time (Fig. 1). Water temperature and salinity was also measured  
153 during each water sampling.

154

155 **2.4 Nitrate  $\delta^{15}\text{N}$  and  $\delta^{18}\text{O}$  Isotope Analysis**

156 Surface samples for  $\delta^{15}\text{N}\text{-NO}_3^-$  and  $\delta^{18}\text{O}\text{-NO}_3^-$  isotopes of dissolved nitrate were  
157 filtered (0.45  $\mu\text{m}$ ), frozen, and shipped to the UC Davis Stable Isotope Facility (SIF) for  
158 analysis. The isotope composition of nitrate was measured following the denitrifier  
159 method (Casciotti et al., 2002; Sigman et al., 2001). In brief, denitrifying bacteria are



160 used to convert nitrate in samples to  $\text{N}_2\text{O}$  gas, which is collected and sent through a mass  
161 spectrometer for determination of the stable isotopic ratios for N and O of nitrate ( $^{15}\text{N}/^{14}\text{N}$   
162 and  $^{18}\text{O}/^{16}\text{O}$ ). Values for  $\delta^{15}\text{N}\text{-NO}_3^-$  and  $\delta^{18}\text{O}\text{-NO}_3^-$  are reported as per mil (‰) relative  
163 to atmospheric  $\text{N}_2$  ( $\delta^{15}\text{N}$ ) or Vienna Standard Mean Ocean Water (VSMOW) ( $\delta^{18}\text{O}$ ),  
164 according to  $\delta^{15}\text{N}$  or  $\delta^{18}\text{O}$  (‰) =  $[(\text{R})_{\text{sample}} / (\text{R})_{\text{standard}} - 1] \times 1000$ , where R denotes  
165 the ratio of the heavy to light isotope ( $^{15}\text{N}/^{14}\text{N}$  or  $^{18}\text{O}/^{16}\text{O}$ ). For data correction and  
166 calibration UC Davis SIF uses calibration nitrate standards (USGS 32, USGS 34, and  
167 USGS 35) supplied by NIST (National Institute of Standards and Technology,  
168 Gaithersburg, MD). The long-term standard deviation for nitrate isotope samples at UC  
169 Davis SIF is 0.4 ‰ for  $\delta^{15}\text{N}\text{-NO}_3^-$  and 0.5 ‰ for  $\delta^{18}\text{O}\text{-NO}_3^-$ . Previous studies (Kaushal  
170 et al., 2011; Kendall et al., 2007) indicate that the relative amounts of  $\delta^{15}\text{N}\text{-NO}_3^-$  and  
171  $\delta^{18}\text{O}\text{-NO}_3^-$  can be used to determine specific sources of nitrate (i.e. fertilizer, nitrification,  
172 atmospheric, or sewage derived nitrate).

173         It should be noted that while the denitrifier method converts sample  $\text{NO}_3^-$  and  
174  $\text{NO}_2^-$  to  $\text{N}_2\text{O}$  gas, in marine systems,  $\text{NO}_2^-$  has been shown to complicate interpretations  
175 of the N and O isotopes of  $\text{NO}_3^-$  if it remains unaccounted for (e.g. Fawcett et al., 2015;  
176 Marconi et al., 2015; Rafter et al., 2013; Smart et al., 2015). This is partially because  
177 during the reduction of  $\text{NO}_3^-$  and  $\text{NO}_2^-$  to  $\text{N}_2\text{O}$  by the denitrifiers, the O isotope effects  
178 are different (and thus need to be corrected for). In addition, the  $\delta^{15}\text{N}$  of  $\text{NO}_2^-$  can be  
179 extremely different from that of  $\text{NO}_3^-$ , potentially further complicating interpretation of  
180 the data.

181



## 182 2.5 Nitrate Isotope Mixing Model

183 To distinguish between the different potential nitrate sources we used a Bayesian  
184 isotope mixing model (Parnell et al., 2010; Parnell et al., 2013; Xue et al., 2012; Yang  
185 and Toor, 2016). For the Bayesian isotope mixing model, the Stable Isotope Analysis in  
186 R (SIAR) package was used to determine the fraction of nitrate in each sample from four  
187 different sources: wastewater, atmospheric, nitrification, and nitrate fertilizer (Parnell et  
188 al., 2010; Parnell et al., 2013; Xue et al., 2012; Yang and Toor, 2016). The SIAR mixing  
189 model is able to incorporate uncertainty in nitrate source estimates based on the  
190 uncertainty in the nitrate source endmembers (see below) (Parnell et al., 2010; Parnell et  
191 al., 2013; Xue et al., 2012; Yang and Toor, 2016).

192 Nitrate source end-member values, for  $\delta^{15}\text{N-NO}_3^-$  and  $\delta^{18}\text{O-NO}_3^-$  were obtained  
193 from the literature, except wastewater nitrate, which was obtained from this study. The  
194 end-member values for  $\delta^{15}\text{N-NO}_3^-$  and  $\delta^{18}\text{O-NO}_3^-$  were  $-10.3\pm 1.7$  and  $10.1\pm 1.5$ ,  
195 respectively for nitrate from nitrification (Mayer et al., 2001),  $0\pm 3$  and  $22\pm 3$ , respectively  
196 for  $\text{NO}_3^-$  fertilizer (Mayer et al., 2002), and  $3\pm 3$  and  $69\pm 5$ , respectively for atmospheric  
197 nitrate (Burns and Kendall, 2002; Divers et al., 2014). The wastewater  $\delta^{15}\text{N-NO}_3^-$  and  
198  $\delta^{18}\text{O-NO}_3^-$  end-member values ( $31.5\pm 7.8$  and  $11\pm 4.5$ , respectively) were based on  
199 averaging the effluent nitrate isotope values measured monthly from Blue Plains during  
200 the study period. The nitrification source represents  $\text{NO}_3^-$  from nitrification in the water  
201 as well as nitrification of ammonia fertilizer in the watershed. The fertilizer source  
202 represents synthetically produced  $\text{NO}_3^-$  fertilizer, not the more common ammonia  
203 fertilizer.



204           Due to the variability in nitrate source endmembers, the mixing model was used  
205 primarily for illustrative purposes and should be viewed with caution (particularly with  
206 regard to identifying other sources besides wastewater). For example, there is high  
207 variability in the nitrification source endmembers because nitrate from nitrification can  
208 come from ammonia fertilizer, manure fertilizer, particulate organic matter within the  
209 water column, etc. The nitrate from nitrification will therefore carry a range of nitrate  
210 isotope values reflecting its original source (Kendall et al., 2007). Additionally, because  
211 denitrification is known to cause the increase in  $\delta^{15}\text{N-NO}_3^-$  and  $\delta^{18}\text{O-NO}_3^-$  values through  
212 isotopic fractionation in approximately a 2:1 relationship (Divers et al., 2014; Kendall et  
213 al., 2007), this isotopic enrichment can complicate the identification of wastewater  
214 nitrate. As a result, water samples with increased wastewater nitrate, based on the mixing  
215 model, may also suggest denitrification has played a role in the isotopic levels of the  
216 sample nitrate.

217

## 218 **2.6 Salinity vs. Nitrate Concentration and Isotope Mixing Plots**

219

220           An additional method using plots of salinity vs.  $\text{NO}_3^-$  concentration or  $\text{NO}_3^-$   
221 isotopes was used to assess whether there is conservative mixing (dilution), or mixing  
222 with additional  $\text{NO}_3^-$  sources down-estuary, or losses of  $\text{NO}_3^-$  through biotic uptake or  
223 denitrification (Middelburg and Nieuwenhuize, 2001; Wankel et al., 2006). Mixing line  
224 equations for  $\text{NO}_3^-$  concentrations were based on equations 1-3 from Middelburg and  
225 Nieuwenhuize (2001) and isotopes mixing lines were based on equation 4 from  
226 Middelburg and Nieuwenhuize (2001). The mixing line equations and endmember  
227 values used for salinity and nitrate isotopes are provided in supporting information (Table



228 S2). Based on those equations, the salinity vs.  $\text{NO}_3^-$  concentration mixing lines are linear,  
229 while the mixing lines for  $\text{NO}_3^-$  isotopes are non-linear (Middelburg and Nieuwenhuize,  
230 2001). Wankel et al. (2006) suggests that when nutrient concentrations fall above the  
231 mixing line this indicates an additional source to raise the concentrations, while  
232 concentrations that fall below the mixing line indicate there is a nutrient sink (e.g.,  
233 denitrification, assimilation, etc.). For nitrate isotopes, when the  $\delta^{15}\text{N}-\text{NO}_3^-$  and  $\delta^{18}\text{O}-$   
234  $\text{NO}_3^-$  values fall above this mixing line, this could indicate an additional source or the  
235 fractionation of nitrate from assimilation or denitrification that would increase the heavy  
236 isotope levels, while isotope values below the mixing line could indicate an additional  
237 source of nitrate with lighter isotope values, such as from nitrification or fertilizer sources  
238 (Wankel et al., 2006).

239

## 240 2.7 Estuarine Nitrogen Net Fluxes

241 A box model was used to estimate net fluxes of TN,  $\text{NO}_3^-$ , and nitrate isotope  
242 loads along the Potomac River Estuary using methods modified from Officer (1980),  
243 Boynton et al. (1995), Hagy et al. (2000), and Testa et al. (2008), which are widely used  
244 methods for tracking nutrient fluxes in estuaries between different salinity zones. First,  
245 the Potomac Estuary was divided into 6 boxes in order to accommodate adequate  
246 sampling stations per box, and to evaluate net fluxes at key locations along the estuarine  
247 gradient (Fig. 2). Next, due to the Potomac Estuary having a semi-diurnal tidal cycle,  
248 where there is movement back and forth across boundaries of the box model, mean  
249 monthly freshwater discharge inputs to the first box (USGS, 2014) and interpolated  
250 salinity values (measured monthly from surface and bottom waters throughout the



251 system) were used to calculate advective and diffusive exchanges of water and salt  
252 between adjacent boxes. Salt balances were then used to compute net exchanges at the  
253 boundaries of the six model boxes, similar to previous estuarine box model studies (e.g.  
254 Boynton et al., 1995; Hagy et al., 2000). Average monthly TN,  $\text{NO}_3^-$  and  $\text{NO}_3^-$  isotope  
255 concentrations (collected from the surface and bottom water at each station, except for  
256  $\text{NO}_3^-$  isotopes, which were collected from the surface only) were multiplied by net  
257 estimated exchange values at the box boundaries and summed to calculate the N load  
258 leaving or entering each box. In order to calculate the loads for  $\text{NO}_3^-$  isotopes, the  $\delta^{15}\text{N}$ -  
259  $\text{NO}_3^-$  and  $\delta^{18}\text{O}$ - $\text{NO}_3^-$  values in per mil (‰) were converted to concentrations ( $\mu\text{g/L}$ ) by  
260 multiplying the  $\text{NO}_3^-$  concentration of the sample by R, the ratio of the heavy to light  
261 isotope ( $^{15}\text{N}/^{14}\text{N}$  or  $^{18}\text{O}/^{16}\text{O}$ ). Fluxes were estimated for each month during the sampling  
262 period and then averaged to find seasonal estimates of N fluxes for the Potomac. The  
263 box model results were used to compute: (1) the total inputs of N, (2) the % inputs of  
264 loads from Blue Plains, (3) the net export of N to the Chesapeake Bay, (4) the % of Blue  
265 Plains inputs that are exported, (5) the net loss in loads along the estuary, and (6) the  
266 contribution of N loads from the Chesapeake Bay through tidal inflow.

267 To account for uncertainty in monthly load estimates, error propagation was used  
268 for each of the hydrologic and nutrient inputs to the model. For example, the error in  
269 discharge data came from averaging the mean daily discharge for each month, the error in  
270 water concentrations came from averaging the surface and bottom water concentrations,  
271 and the error in N from atmospheric deposition came from averaging the weakly  
272 deposition data for each month. These uncertainties in the inputs to the box model were



273 then propagated for each of the box model calculations, similar to Filoso and Palmer  
274 (2011).

275 Inputs to the box model include, total monthly precipitation data based on  
276 averaging data from three stations along the Potomac Estuary (Precipitation data is from  
277 the NOAA National Centers for Environmental Information, Climate Data Online),  
278 monthly estimates of atmospheric deposition for  $\text{NH}_4^+$ ,  $\text{NO}_3^-$ , and DIN (obtained from the  
279 National Atmospheric Deposition Program / National Trends Network),  $\text{NO}_3^-$   
280 concentrations and isotope levels in atmospheric deposition (from Buda and DeWalle,  
281 2009, for the nearby central Pennsylvania region for the year 2005, which was a similar  
282 year hydrologically (as described below)), N inputs from the land (from Chesapeake Bay  
283 model output from 2005), surface and bottom water nutrient and salinity concentrations  
284 (from MD DNR), and inputs from the Blue Plains wastewater treatment plant. Also,  
285 while there are no USGS gages located along the Potomac Estuary, there is one USGS  
286 gage (USGS 01646580) located directly above the Estuary, above the fall line (the  
287 location where the hydrodynamics of the river cease being tidally influenced) and this  
288 gage was used to account for freshwater inputs into the first box. The model also takes  
289 into account water temperature and evaporation.

290 For the box model it is assumed that the 14 other WWTPs further down-estuary  
291 have little effect on the nitrate signal because their combined TN load is 32% of the TN  
292 from Blue Plains and for the other reasons described below. While  $\delta^{15}\text{N}-\text{NO}_3^-$  and  $\delta^{18}\text{O}-$   
293  $\text{NO}_3^-$  isotope values were not measured directly for the 14 other down-estuary wastewater  
294 treatment plants, based on the literature, the values of these isotopes are typically lower  
295 ( $\sim 10\text{‰}$  for  $\delta^{15}\text{N}-\text{NO}_3^-$  and  $\sim 0$  for  $\delta^{18}\text{O}-\text{NO}_3^-$ ) compared to  $31.5\text{‰}$  for  $\delta^{15}\text{N}-\text{NO}_3^-$  and



296 11‰  $\delta^{18}\text{O}-\text{NO}_3^-$  for Blue Plains (Kendall et al., 2007; Wang et al., 2013; Wankel et al.,  
297 2006). As a result, we expected the other WWTPs to have a similar or an even less  
298 pronounced wastewater isotope signal compared to Blue Plains, which has biological  
299 nitrogen removal (i.e. denitrification is promoted within the WWTP), elevating the  $\delta^{15}\text{N}-$   
300  $\text{NO}_3^-$  and  $\delta^{18}\text{O}-\text{NO}_3^-$  isotope values at Blue Plains more (Kendall et al., 2007).  
301 Consequently, the estimated nitrate loads down-estuary incorporate Blue Plains and  
302 nitrate inputs from the other WWTPs, and are considered conservative estimates because  
303 the additional WWTPs only add to the TN loads and  $\text{NO}_3^-$  isotope signals and thus lessen  
304 the decline in loads or isotope values down estuary.

305 A second assumption was made for the box model related to estuarine mixing.  
306 Although portions of the lower estuary can be seasonally stratified, we assumed each box  
307 to be well mixed vertically as no bottom water isotope values were available to constrain  
308 a 2-layer box model. This assumption is supported by other bottom water data that is  
309 available and by samples taken along the width of the estuary. For example, we have  
310 conducted the box model and other analyses with and without bottom water isotope data  
311 and found minimal change in results (Fig. S1, see below). Our measurements of various  
312 biogeochemical signatures at the station close to the estuarine turbidity maximum  
313 suggests that there is intense mixing at this site, and prior studies have documented  
314 extensive mixing in the freshwater tidal portion of the system (Elliott, 1976, 1978;  
315 Pritchard, 1956). Also, it can be assumed that because wastewater effluent inputs are  
316 freshwater, much of the effluent plume would likely not sink in the more dense estuarine  
317 waters moving up from the bay. Additionally, our box model estimates of net fluxes was  
318 compared to a complex, 3 dimensional hydrodynamic model (described below) that



319 incorporates stratification, and this comparison provided support for the low impact of  
320 assuming mixing in our approach.

321 While seasonal stratification has been found close to the mouth of the of the  
322 Potomac estuary (Hamdan and Jonas, 2006), using documented nitrate bottom water  
323 isotope values from near the mouth of the estuary (Horrigan et al., 1990) we calculate  
324 that incorporating bottom water isotope values would have a minimal impact on the flux  
325 estimates of our box model, particularly when not including spring 2011 (Fig. S1). But  
326 when including spring 2011, and using the reported values of 10‰ for bottom water  
327  $\delta^{15}\text{N-NO}_3^-$ , based on Horrigan et al. (1990), in Boxes 5 and 6 where stratification is most  
328 likely, our estimates for the flux of  $\delta^{15}\text{N-NO}_3^-$  from these boxes increases by 20% on  
329 average, and the net loss in load from box 1 to box 6 increases by 12% on average. This  
330 indicates that our estimates are conservative because by not using bottom water we  
331 estimate a smaller net loss in  $\delta^{15}\text{N-NO}_3^-$  (Fig. S1).

332 For the box model we also assumed the estuary to be well mixed laterally. In  
333 terms of potential variability for samples taken at different locations along the width of  
334 the estuary, there was found for surface water samples, on average, a  $6\pm 3\%$  difference in  
335  $\delta^{15}\text{N-NO}_3^-$ , a  $7\pm 3\%$  difference in  $\delta^{18}\text{O-NO}_3^-$ , a  $24\pm 8\%$  difference in  $\text{NO}_3^-$ , and a  $15\pm 3\%$   
336 difference in TN (based on samplings that were done at two or more locations along the  
337 same longitudinal transect at approximately the same distance down-estuary, but at  
338 different locations horizontally at that location). Based on this, the nitrate isotopes values  
339 and  $\text{NO}_3^-$  and TN concentrations appear to show that the estuary is fairly well mixed  
340 laterally.



341 To assess the accuracy of the box model assumptions and results, estimated net  
342 fluxes of total N were compared to simulation output from the Chesapeake Bay Water  
343 Quality Model. This model was developed by the U.S. EPA to aid in efforts to set  
344 TMDLs for the Chesapeake Bay (Cercio et al., 2010), and combines a 3-D hydrodynamic  
345 model (CH3D) with a water quality model (CE-QUAL-ICM). Simulation output data  
346 were available for 1996, 2002, and 2005. We selected a simulation year (2005) because  
347 it had similar river discharge conditions to 2010, and compared modeled net fluxes of TN  
348 at three boundary locations to estimates at the same (or nearby) box model boundaries.

349

## 350 **2.8 Statistical Analyses**

351 Statistical analyses were performed using the statistical package R (R  
352 Development Core Team, 2013). Linear regression was used to test for significant  
353 changes in stream chemistry and nitrate isotope data with distance down estuary.  
354 Repeated measures analysis of variance (ANOVA) was used to test for seasonal  
355 differences in nitrate isotopes trends with distance.

## 356 **3 Results**

### 357 **3.1 Spatial and Temporal Trends in N Concentrations**

358 Longitudinal patterns of dissolved inorganic nitrogen (DIN) in the lower  
359 Potomac River showed an increase in concentrations near and directly below the Blue  
360 Plains wastewater treatment plant and then a steady decline in concentrations down to the  
361 Chesapeake Bay (Fig. 3a). The implementation of tertiary treatment in 2000 coincided  
362 with a significant drop in annual average DIN concentration directly down-estuary (from



363  $1.7 \pm 0.02$  to  $1.3 \pm 0.01$  mg/l,  $p < 0.05$ ) (Fig. 3a), when comparing years directly prior  
364 (1997-1999) and the years directly after 2000 (2001-2005). However, the impact of the  
365 wastewater treatment plant improvements on reducing longitudinal patterns of DIN was  
366 only apparent for the first 30 km down-estuary. After this, both the pre- and post-2000  
367 DIN concentrations overlapped (Fig. 3a). As DIN decreased longitudinally down-estuary  
368 of the wastewater treatment plant, there was also a small, but significant increase in total  
369 organic nitrogen (TON) after the year 2000 ( $p < 0.01$ , Fig. 3a), not including the last  
370 sample near the mouth of the estuary, which is likely influenced by tidal inflow.

371           There were seasonal variations in DIN concentrations along the Potomac River  
372 Estuary with the greatest concentrations in the winter and spring (Fig. 3b). There is also  
373 a steeper decline in DIN with distance during fall, winter, and summer compared to the  
374 spring ( $p < 0.05$ , Fig. 3b). The average molar ratio of DIN to  $\text{PO}_4^{3-}$  (N:P ratio) showed  
375 an initial increase, then a decrease as estuarine salinity started to increase (Fig. 3c).  
376 During the summer and fall, the N:P ratio fell below the Redfield ratio (16:1, the atomic  
377 ratio of nitrogen and phosphorus found in oceans and phytoplankton), around 40 km  
378 down-estuary and stayed below 16, which indicated a shift from P to N limitation.  
379 During the winter and spring, the N:P ratio never fell below 16 and increased steadily  
380 after 50 km down-estuary (Fig. 3c). There was also a significant negative relationship  
381 between  $\text{NO}_3^-$  and DOC concentration during the study period ( $p < 0.01$ , Fig. 4).

382

### 383 **3.2 Spatial and Seasonal Trends in $\text{NO}_3^-$ Isotopes and Sources**

384           During each season, except spring,  $\delta^{15}\text{N-NO}_3^-$  values increased sharply at the  
385 Blue Plains outfall, from  $9.3 \pm 1.4$  ‰ up-estuary to  $25.7 \pm 2.9$  ‰ at the outfall ( $p < 0.05$ ),



386 and then rapidly decreased within 2 km down-estuary to  $15.7 \pm 2.2$  ‰ ( $p < 0.05$ , Fig. 5a).  
387 During the summer and fall, the  $\delta^{15}\text{N-NO}_3^-$  values showed the largest increase near the  
388 effluent outfall (except for one very high winter value) and then a significant decrease ( $p$   
389  $< 0.05$ ) with distance down-estuary. There was also a slight increase in  $\delta^{15}\text{N-NO}_3^-$  and  
390  $\delta^{18}\text{O-NO}_3^-$  values from 1 to 6 km down-estuary (Fig. 5a,b). During the winter and spring,  
391 the  $\delta^{15}\text{N-NO}_3^-$  and  $\delta^{18}\text{O-NO}_3^-$  values remained relatively constant throughout the estuary,  
392 even near Blue Plains (Fig. 5a,b), while during the summer and fall the  $\delta^{15}\text{N-NO}_3^-$  and  
393  $\delta^{18}\text{O-NO}_3^-$  values steadily declined after 6-10 km down-estuary (Fig. 5a,b). At the mouth  
394 of the estuary, the  $\delta^{15}\text{N-NO}_3^-$  values for all seasons were roughly equivalent (Fig. 5a).  
395 During the summer and fall, the  $\delta^{18}\text{O-NO}_3^-$  values showed a steady decrease after 12 km  
396 down-estuary, while they increased during spring and winter (Fig. 5b).

397         Based on the nitrate isotope mixing model, nitrate contributions from wastewater  
398 ranged from  $80 \pm 13\%$  at the wastewater outfall to  $57 \pm 11\%$  within the first 1 km down-  
399 estuary. Wastewater nitrate contributions then decreased to  $44 \pm 14\%$  at the confluence  
400 of the Potomac River Estuary with Chesapeake Bay (Fig. 5c). Nitrate from nitrification  
401 (of N from upriver manure or ammonia fertilizer and also Blue Plains wastewater N)  
402 increased from  $13 \pm 12\%$  at the wastewater outfall to  $29 \pm 22\%$  at the confluence of the  
403 Potomac River Estuary with Chesapeake Bay (Fig. 5c). Nitrate from fertilizer increased  
404 from  $6 \pm 6\%$  at the wastewater outfall to  $22 \pm 22\%$  at the confluence of the Potomac  
405 River Estuary with Chesapeake Bay (Fig. 5c). Nitrate from atmospheric deposition  
406 changed little along the Potomac Estuary from  $1 \pm 1$  at the wastewater outfall to  $5 \pm 5$  at  
407 the confluence with the Chesapeake Bay (Fig. 5c). At the last two sampling stations near



408 the mouth of the Potomac River Estuary,  $\text{NO}_3^-$  from fertilizer showed an increase, while  
409  $\text{NO}_3^-$  from nitrification showed a corresponding decline (Fig. 5c).

410

### 411 3.3 $\delta^{15}\text{N}\text{-NO}_3^-$ and $\delta^{18}\text{O}\text{-NO}_3^-$ , $\text{NO}_3^-$ Concentration, and Salinity Relationships

412 The Blue Plains effluent and Potomac River samples within 20 km downriver of  
413 the wastewater treatment plant showed a significant positive relationship between  $\delta^{15}\text{N}\text{-NO}_3^-$   
414  $\text{NO}_3^-$  and  $\delta^{18}\text{O}\text{-NO}_3^-$  ( $p < 0.05$ ) (Fig. 6a). When denitrification and biotic uptake occurs,  
415 plotting  $\delta^{15}\text{N}\text{-NO}_3^-$  vs.  $\delta^{18}\text{O}\text{-NO}_3^-$  shows a 2:1 relationship (Kendall et al. 2007). The  
416 Blue Plains effluent samples showed approximately a 2.4 to 1 relationship. The samples  
417 within 20 km downriver showed a 3:1 ratio (Fig. 6a). The nitrate samples within the first  
418 6 km showed a 2.4 to 1 relationship (Fig. 6a). There were also seasonal differences in the  
419 relationship between  $\delta^{15}\text{N}\text{-NO}_3^-$  and  $\delta^{18}\text{O}\text{-NO}_3^-$  (Fig. 6b); spring, summer, and fall were  
420 characterized by close to a 2:1 relationship between  $\delta^{15}\text{N}\text{-NO}_3^-$  vs.  $\delta^{18}\text{O}\text{-NO}_3^-$ , while  
421 winter showed a ~8:1 relationship.

422 Because salinity is a conservative tracer, plots of salinity vs.  $\text{NO}_3^-$ ,  $\delta^{15}\text{N}\text{-NO}_3^-$ , and  
423  $\delta^{18}\text{O}\text{-NO}_3^-$  can indicate effects of mixing between water at the tidal freshwater section  
424 with water from the mesohaline section of the Potomac River Estuary. Deviations from  
425 the mixing lines can indicate additional sources or biological transformations  
426 (Middelburg and Nieuwenhuize, 2000; Wankel et al., 2006). Surface water  $\text{NO}_3^-$   
427 concentrations and nitrate isotopes fell on (for  $\delta^{18}\text{O}\text{-NO}_3^-$ ) or slightly below mixing line  
428 (for  $\delta^{15}\text{N}\text{-NO}_3^-$ ) during the spring (Fig. 7a,b,c), which indicated mostly conservative  
429 mixing (dilution or inputs from low  $\delta^{15}\text{N}\text{-NO}_3^-$  like nitrification, see discussion below).  
430 But during the summer and fall, the  $\text{NO}_3^-$  concentration and isotope values fell well



431 below the mixing lines. During the winter, the values fell both above and below the  
432 mixing line (Fig. 7a,b,c), which indicated non-conservative mixing (please see discussion  
433 below).

434

### 435 **3.4 Spatial and Seasonal Trends in N Loads**

436 Our comparisons of box model net exchange estimates with simulation output  
437 provided by the Chesapeake Bay Program Eutrophication Model (“Bay Model”) revealed  
438 similar TN loads between our results and the Bay Model in the winter, spring, and fall,  
439 with the largest differences in the models evident in the summer months at the boundary  
440 location where tidal fresh transitions to oligohaline conditions and at the mouth of the  
441 estuary (Table S3 and Figures 8 and 9). Even so, these differences are smaller than a  
442 factor of 2 for winter and spring and for most of the summer and fall, despite the  
443 assumption of complete mixing in our box model, a good agreement considering the  
444 simplification of hydrodynamics inherent to a box modeling approach when compared to  
445 the highly constrained CH3D hydrodynamic modeling platform (Cerco et al., 2010). The  
446 Potomac estuary is well mixed along two thirds of its length, and this likely contributes to  
447 our success in applying a single layer box model to this system. The box model also  
448 permitted estimates of TN loads at smaller spatial scales than the three boundaries  
449 available from the Chesapeake Bay Program, which could enable a better interpretation  
450 of where Blue Plains effluent was subject to transformations in the oligohaline portion of  
451 the estuary (Fig. 8). The caveat here is that box-modeled summer loads should be  
452 interpreted with caution because they show the greatest differences from the CH3D  
453 model.



454 Results of the box model indicated that the net load (kg/day) of TN,  $\text{NO}_3^-$ , and  
455  $\delta^{15}\text{N}\text{-NO}_3^-$  decreased down-estuary during each season (Fig. 10a-c,  $p < 0.05$  for winter  
456 and spring and  $p < 0.1$  for summer and fall). N loads were highest along the estuary  
457 during spring and winter (Fig. 10), and there was a greater decline in TN loads on  
458 average from box 1 to box 6 during winter and spring (a loss of  $\sim 27,000 \pm 15,000$  and  
459  $50,000 \pm 52,000$  kg/day, respectively) (Table 1) compared to summer and fall (a loss of  
460  $\sim 7,000 \pm 8,000$  and  $15,000 \pm 13,000$  kg/day, respectively). However, the summer and  
461 fall months showed a greater percent decline in TN ( $75 \pm 75\%$  and  $112 \pm 95\%$ ,  
462 respectively) compared to winter and spring ( $54 \pm 40$  and  $36 \pm 43\%$ , respectively). The  
463 relatively high errors are primarily from the larger uncertainty found in the last box, at the  
464 mouth of the estuary, due to the larger size of this box and greater uncertainty in fluxes at  
465 the mouth of the estuary; the uncertainties are much smaller further up-estuary (See Fig.  
466 10a).  $\text{NO}_3^-$  and  $\delta^{15}\text{N}\text{-NO}_3^-$  follow the same seasonal patterns as TN. Also, winter, along  
467 with summer and fall, showed a greater percent decline in  $\text{NO}_3^-$  and  $\text{NO}_3^-$  isotope loads  
468 compared to spring (Table 1).

469 Using an estimated N burial rate of  $7.09 \times 10^6$  kg/yr (which is an average of burial  
470 rate estimates for the upper and lower Potomac Estuary) from Boynton et al. (1995), it  
471 was calculated that, on an mean annual basis, burial accounts for about 77% of the loss in  
472 TN. Denitrification was then calculated, by difference, to account for the remaining 23%  
473 loss in TN load. Using a different independent method, based on the average annual  
474 estimated denitrification rate ( $2.8 \times 10^6$  kg/yr) from the upper and lower Potomac  
475 (Boynton et al., 1995), and the box model results, it is estimated that denitrification



476 accounts for about 27% of the TN removal. Consequently denitrification is estimated to  
477 account for 23 to 27% of the loss in TN load along the Potomac Estuary.

478         The percent contribution of TN inputs from the Blue Plains wastewater treatment  
479 to the main stem of the Chesapeake Bay ranged from 8 to 47 % (Table 1). The  
480 contribution was significantly lower during the winter and spring ( $10 \pm 13$  and  $8 \pm 1\%$ ,  
481 respectively) compared to summer and fall ( $38 \pm 3$  and  $47 \pm 13\%$ , respectively, Table 1),  
482 when TN fluxes from all sources are relatively low. The percent contribution of Blue  
483 Plains wastewater TN inputs, which are exported to the Chesapeake Bay ranged from <4  
484 to 71%, and they were highest in the spring ( $71 \pm 20\%$ , Table 1). There were also N  
485 inputs to the Potomac river-estuarine continuum from the Chesapeake Bay during each  
486 season, except spring, due to higher flows (Table 1 & 2) because flow in spring was too  
487 high to allow the inputs from the Bay that occurred in the other seasons.  $\text{NO}_3^-$  and  $\delta^{15}\text{N}$ -  
488  $\text{NO}_3^-$  follow the same seasonal patterns as TN, showing the greatest percentage of inputs  
489 from Blue Plains exported during the spring.

490

#### 491 **4 Discussion**

492         While coastal urbanization can have a major impact on water quality in receiving  
493 waters, the results of this study suggest that estuaries also show a large capacity to  
494 transform or bury anthropogenic N. In particular, our results suggest that 30-96% of  
495 inputs of N from the Washington D.C. Blue Plains wastewater treatment plant were  
496 removed *via* burial or denitrification along the Potomac river-estuarine continuum,  
497 depending on the season (Table 1). Recent work shows that urban watersheds and river



498 networks can also be “transformers” of nitrogen across similar broad spatial scales, which  
499 impacts downstream coastal water quality (Kaushal et al., 2014a). Here, we show that  
500 the urban river-estuarine continuum also acts as a transformer and can have large impacts  
501 on the sources, amounts, and forms of nitrogen transported to the Chesapeake Bay. Our  
502 results showed that N transformation varied across seasons and hydrologic conditions  
503 with important implications for anticipating changes in sources and transport of coastal  
504 nitrogen pollution in response to future climate change. This is particularly significant,  
505 given long-term increases in warming water temperatures of major rivers and increased  
506 frequency and magnitude of droughts and floods in this region and elsewhere (e.g.  
507 Kaushal et al., 2010a; Kaushal et al., 2014b).

508

#### 509 **4.1 Spatial and Temporal Trends in N Concentrations and Loads**

510 The decrease in DIN concentrations with distance down-estuary is largely from  
511 denitrification, assimilation, and burial, as indicated by the inverse relationship between  
512  $\text{NO}_3^-$  concentrations and DOC and TON concentrations, the  $\text{NO}_3^-$  isotope data, and N  
513 mass balance data discussed below. Dilution from tidal marine waters plays a minor role  
514 in the decrease in DIN and the incoming tidal waters may even contribute to DIN as  
515 suggested by the decrease in DIN slope after 130 km down estuary (Boynton et al.,  
516 1995), depending on the season. The installation of tertiary wastewater treatment  
517 technology at Blue Plains in the year 2000 showed a significant drop in DIN  
518 concentrations within 20-30 km of Blue Plains. However, the DIN concentrations below  
519 30 km down-estuary were approximately the same based on an annual average, before  
520 and after the year 2000. One explanation is that the dissolved wastewater N is



521 completely assimilated into particulate organic matter (supported by the inverse  $\text{NO}_3^-$  vs.  
522 TON or DOC relationships (Fig.s 3a and 4) or removed by denitrification (as suggested  
523 by the isotope data discussed below) within the first 10 km down-estuary, and thus the  
524 majority of DIN below 30 km is from other inputs than the Blue Plains wastewater  
525 treatment plant. For example, there are 14 other smaller wastewater treatment plants  
526 along the Potomac River Estuary, which contribute a total of about 270 mgd (almost as  
527 much as the amount Blue Plains contributes). Also, our isotope mixing model data  
528 (discussed more below) suggests nitrification (likely of upriver manure or ammonia  
529 fertilizer inputs) and fertilizer are important sources further down-estuary; and 42% of the  
530 land-use along the Potomac Estuary is agriculture (Karrh et al., 2007b). A second  
531 explanation could be related to a change in N:P ratio with distance down-estuary.  
532 Specifically, there was a rise in estuarine salinity around 30 to 50 km down-estuary and a  
533 coinciding increase in dissolved  $\text{PO}_4^{3-}$  concentration (typical of the estuarine salinity  
534 gradient) (Jordan et al., 2008). When the N:P ratio fell below the Redfield Ratio of 16:1,  
535 the estuary could shift from P limitation to N limitation (Fisher et al., 1999). The  
536 potential shift from P to N limitation occurred 40-50 km down-estuary, around the  
537 estuarine turbidity maximum, which is associated with higher estuarine bacterial  
538 productivity (Crump and Baross, 1996), and may be driving DIN removal further down-  
539 estuary.

540 Mass balance indicates that TN and  $\text{NO}_3^-$  loads decreased down-estuary each  
541 season (despite inputs from the 14 other wastewater treatment plants down-estuary). On  
542 an annual average, it was estimated that approximately 23-27% of the loss in TN could be  
543 attributed to denitrification, while 73-77% was lost through burial into the estuarine



544 sediment. This is supported by the  $\text{NO}_3^-$  isotope data indicating that there was likely  
545 denitrification (an assimilation) of  $\text{NO}_3^-$ , particularly within 6 km down-estuary from the  
546 Blue Plains wastewater treatment plant (discussed further below). Over seasonal time  
547 scales, there was a greater percent decline in TN loading during summer and fall, likely  
548 due to warmer temperatures and increased biological transformation (attributable to high  
549 rates of phytoplankton uptake, detrital deposition, and remineralization for subsequent  
550 recycling) (Eyre and Ferguson, 2005; Gillooly et al., 2001; Harris and Brush, 2012;  
551 Nowicki, 1994), which suggested that the urban river-estuarine continuum may be more  
552 efficient at removing TN during the summer and fall. Compared to summer and fall,  
553 winter also had a relatively high percent decline in  $\text{NO}_3^-$  loads possibly driven by the  
554 higher concentrations typically found in winter months, which could result in quicker  
555 assimilation through first order reaction rate kinetics (Betlach and Tiedje, 1981). Since  
556 there was no evidence for denitrification during the winter, burial could also be a  
557 mechanism for the relative high decline in winter months, which is typical of higher  
558 flows (Boynton et al., 1995; Milliman et al., 1985; Sanford et al., 2001). However, more  
559 work is necessary to evaluate the fate of nitrate using ecosystem process level  
560 measurements.

561         The higher total exports of TN and  $\text{NO}_3^-$  to Chesapeake Bay during the winter and  
562 spring are due to greater N inputs from the upper and lower watershed and/or greater  
563 flow rates. The proportion of N exports attributed to Blue Plains wastewater treatment  
564 plant were the highest in the spring, likely due to lower water residence times (Table 2),  
565 resulting in less time for biological uptake, removal, or burial of N. The greater decline  
566 in N loads during the spring, however, may be attributed to multiple factors, such as



567 greater N loads being imported from the upper estuary and higher concentrations,  
568 compared to summer and fall (Table 1) and thus driving greater losses (from burial and  
569 denitrification) due to first order reaction rate kinetics (Betlach and Tiedje, 1981) similar  
570 to winter (described above), stratification that is characteristic of higher flows (Boesch et  
571 al., 2001), and increased burial rates due to greater sediment loads during higher flows  
572 (Milliman et al., 1985; Sanford et al., 2001). As mentioned previously, more work is  
573 necessary regarding linking ecosystem processes and microbial dynamics with the fate of  
574 nitrate in the estuary. Nonetheless, the decline in TN and  $\text{NO}_3^-$  loads down-estuary each  
575 season provide strong evidence for the transformation and retention of N along estuaries.  
576

577 **4.2 Spatial Trends in  $\text{NO}_3^-$  Sources Indicate Denitrification and Assimilation of**  
578  **$\text{NO}_3^-$  initially Dominates and then Nitrification Dominates Further Down-**  
579 **Estuary**

580 The Potomac River estuary was a transformer of wastewater N inputs from the  
581 Washington D.C. metropolitan area to its confluence with Chesapeake Bay. The values  
582 for  $\delta^{15}\text{N-NO}_3^-$  above the wastewater treatment plant were relatively high, suggesting  
583 upriver sources may primarily be from animal waste (Burns et al., 2009; Kaushal et al.,  
584 2011; Kendall et al., 2007). This is consistent with a previous study, which found that  
585 43% of N inputs to the upper Potomac River are from manure (Jaworski et al., 1992).  
586 Effluent inputs from the Blue Plains wastewater treatment plant significantly increased  
587 the  $\delta^{15}\text{N-NO}_3^-$  values even further, yet this  $\text{NO}_3^-$  signal from wastewater disappeared after  
588 20-30 km down-estuary. The increase in  $\delta^{15}\text{N-NO}_3^-$  and  $\delta^{18}\text{O-NO}_3^-$  values within the first  
589 1 to 6 km down-estuary suggest denitrification or assimilation of nitrate, due to the



590 lighter  $\delta^{14}\text{N-NO}_3^-$  and  $\delta^{16}\text{O-NO}_3^-$  isotopes being preferentially denitrified or assimilated  
591 and leaving behind the heavier nitrate isotopes (Granger et al., 2008; Granger et al., 2004;  
592 Kendall et al., 2007) (see further discussion below). But the gradual decline in both  
593  $\delta^{15}\text{N-NO}_3^-$  and  $\delta^{18}\text{O-NO}_3^-$  values from 6 km to 160 km down-estuary suggests  
594 nitrification dominates this portion of the estuary because the process of nitrification,  
595 which converts ammonia to nitrate results in lighter nitrate isotopes being generated  
596 through fractionation (Kendall et al., 2007; Vavilin, 2014) (see further discussion below).  
597 However, the decline in  $\delta^{15}\text{N-NO}_3^-$  and  $\delta^{18}\text{O-NO}_3^-$  loads corresponding with the decline  
598 in overall  $\text{NO}_3^-$  loads down-estuary also suggests that the heavy nitrate isotopes are being  
599 removed as well as the light isotopes. The disappearance of  $\delta^{15}\text{N-NO}_3^-$  and  $\delta^{18}\text{O-NO}_3^-$   
600 down-estuary where  $\text{NO}_3^-$  concentrations are very low (~0.01 mg/l) may indicate that  
601 assimilation or even denitrification is occurring on the remaining heavy  $\delta^{15}\text{N-NO}_3^-$  or  
602  $\delta^{18}\text{O-NO}_3^-$  after the lighter  $\delta^{14}\text{N-NO}_3^-$  or  $\delta^{16}\text{O-NO}_3^-$  is all used up (Fogel and Cifuentes,  
603 1993; Vavilin et al., 2014; Waser et al., 1998a; Waser et al., 1998b).

604       Seasonal differences in the longitudinal trends for  $\delta^{15}\text{N-NO}_3^-$  and  $\delta^{18}\text{O-NO}_3^-$   
605 suggest differences in biological transformations of nitrate due to differences in water  
606 temperature, hydrology, and/or N inputs. The  $\delta^{15}\text{N-NO}_3^-$  values from effluent inputs  
607 were likely higher in warmer months due to higher denitrification rates in the wastewater  
608 treatment plant associated with warmer water temperatures (Dawson and Murphy, 1972;  
609 Pfenning and McMahon, 1997), resulting in elevated  $\delta^{15}\text{N-NO}_3^-$  values produced by  
610 isotopic fractionation (Kendall et al., 2007; Mariotti et al., 1981). An increase in  $\delta^{15}\text{N-}$   
611  $\text{NO}_3^-$  between 2 and 6 km down-estuary during summer and fall (Fig. 5b) further  
612 suggested increased denitrification or biological uptake due to warmer water



613 temperatures and fractionation (Eyre and Ferguson, 2005; Gillooly et al., 2001; Harris  
614 and Brush, 2012; Nowicki, 1994). The significant drop in  $\delta^{15}\text{N-NO}_3^-$  beyond 10 km  
615 down-estuary during summer and fall may have been due to mixing with other N sources  
616 and increased nitrification (Wankel et al., 2006) (see further discussion below). During  
617 the spring, there was also a significant decline in  $\delta^{15}\text{N-NO}_3^-$  between 10 and 160 km  
618 down-estuary, but this was likely attributed to dilution and nitrification, based on the  
619 conservative mixing results discussed below. The lack of a significant change during the  
620 winter, may be due to shorter residence times (Table 2) and cooler temperatures,  
621 contributing to lower biological transformation rates. Further down-estuary, near the  
622 mouth of the estuary, the increase in  $\delta^{18}\text{O-NO}_3^-$  in winter and spring might indicate  
623 denitrification in the estuary but in spring nitrate seems conservative based on the salinity  
624 mixing plots. The decline in  $\delta^{18}\text{O-NO}_3^-$  down-estuary in summer and fall suggest that  
625 processes other than denitrification in the estuary are controlling the  $\delta^{18}\text{O-NO}_3^-$ , such as  
626 nitrification.

627

### 628 **4.3 Isotope and Salinity Mixing Models Suggest Seasonal Patterns in N**

#### 629 **Transformation Influenced by Temperature and Residence Time**

630 Seasonally, the ~2:1 relationship between  $\delta^{15}\text{N-NO}_3^-$  and  $\delta^{18}\text{O-NO}_3^-$  during  
631 spring, summer and fall, may indicate denitrification or assimilation, but the salinity  
632 mixing plots discussed below suggests no denitrification in the spring. The fact that the  
633  $\delta^{15}\text{N}:\delta^{18}\text{O}$  ratio is between 1 and 2 for summer and fall may suggest assimilation plays a  
634 role, which is supported by previous studies which found a 1:1 relationship for  
635 assimilation in the marine environment (Granger et al., 2004; Karsh et al., 2012; Karsh et



636 al., 2014). However, other previous studies suggest that a  $\delta^{15}\text{N}:\delta^{18}\text{O}$  ratio between 1 and  
637 2 can also be caused by denitrifying bacteria (Granger et al., 2008; Lehmann et al., 2003).  
638 Additionally, the divergence from the 2:1 ratio further down-estuary samples may  
639 indicate mixing between two or more  $\text{NO}_3^-$  sources, such as between atmospheric,  
640 marine, or nitrification (Kaushal et al., 2011; Wankel et al., 2006). Due to water column  
641 dissolved oxygen levels averaging over 4 mg/L (data from Chesapeake Bay program, not  
642 shown), assimilation likely dominates  $\text{NO}_3^-$  removal in the water column, while  
643 denitrification likely dominates nitrate removal from the sediment, which supported by  
644 previous work (Cornwell et al., 2014; Kemp et al., 1990).

645 Denitrification is likely a sink for  $\text{NO}_3^-$  during the summer and fall based on the  
646 increases in  $\delta^{15}\text{N}-\text{NO}_3^-$  and  $\delta^{18}\text{O}-\text{NO}_3^-$  within 6 km down-estuary and due to warmer  
647 water temperatures, while there is no evidence for denitrification in the winter due to  
648 reduced biological activities typical in cooler winter temperatures (Eyre and Ferguson,  
649 2005; Gillooly et al., 2001; Harris and Brush, 2012; Nowicki, 1994). Nevertheless,  
650 nitrate removal was significant in all seasons, including winter suggesting other  
651 mechanisms, as indicated by the salinity based mixing lines.

652 Plots of salinity vs.  $\text{NO}_3^-$ ,  $\delta^{15}\text{N}-\text{NO}_3^-$ , and  $\delta^{18}\text{O}-\text{NO}_3^-$  were used to provide  
653 evidence for conservative mixing, uptake, production, or contributions from other  $\text{NO}_3^-$   
654 sources.  $\text{NO}_3^-$  concentrations fell below the mixing lines during the summer, fall, and  
655 winter, suggesting non-conservative mixing behavior due to the presence of a  $\text{NO}_3^-$  sink,  
656 such as assimilation or denitrification (Wankel et al., 2006). During the spring  $\text{NO}_3^-$   
657 concentrations fell on the mixing line, however, suggesting that there were no important  
658 sources or sinks. This may be due to higher flows and shorter residence times in the



659 spring (Table 2), which can result in less biological transformations of  $\text{NO}_3^-$ . In the  
660 salinity vs.  $\delta^{15}\text{N}-\text{NO}_3^-$  and  $\delta^{18}\text{O}-\text{NO}_3^-$  plots, when the isotope values fell below the  
661 mixing lines, this suggested the contribution of  $\text{NO}_3^-$  from sources with lower  $\delta^{15}\text{N}-\text{NO}_3^-$   
662 and  $\delta^{18}\text{O}-\text{NO}_3^-$ , such as fertilizer inputs or nitrification, which produces nitrate with lower  
663  $\delta^{15}\text{N}-\text{NO}_3^-$  and  $\delta^{18}\text{O}-\text{NO}_3^-$  values through fractionation (Kaushal et al., 2011; Kendall et  
664 al., 2007). An increase in nitrification down-estuary is likely attributed to the conversion  
665 of remineralized N to nitrate or from down-estuary inputs of wastewater ammonia that is  
666 converted to nitrate (Middelburg and Nieuwenhuize, 2001). During the spring,  $\delta^{18}\text{O}-$   
667  $\text{NO}_3^-$ , isotope values again fell mostly on the mixing line, which may indicate the  
668 Potomac River Estuary is acting more like a transporter instead of a transformer (e.g.  
669 Kaushal and Belt, 2012), transporting  $\text{NO}_3^-$  without there being any significant sinks of  
670  $\text{NO}_3^-$  or mixing with additional sources, likely due to lower residence times (Table 2) in  
671 the spring. However, the fact that during the spring the  $\delta^{15}\text{N}-\text{NO}_3^-$  values were slightly  
672 below the mixing line indicates there may have been an increased amount of nitrate  
673 inputs from the watershed through runoff carrying nitrate derived from nitrification.  
674 During the winter,  $\delta^{15}\text{N}-\text{NO}_3^-$  values also fell above the mixing line for some samples,  
675 which suggested the contribution of heavy  $\delta^{15}\text{N}-\text{NO}_3^-$  from an additional down-estuary  
676 source (there are 14 other wastewater treatment plants in the lower Potomac watershed).  
677 This was likely not the case during the summer and fall when other sources and sinks  
678 may dominate due to greater biological activities (Eyre and Ferguson, 2005; Gillooly et  
679 al., 2001; Harris and Brush, 2012; Nowicki, 1994) or during the spring when flows are  
680 higher there is more conservative behavior. Even though only surface water salinity,  
681 nutrient, and isotope values were used in these mixing line plots, when bottom water



682 nutrient and isotope data was averaged with the surface water values, the mixing lines  
683 plots and results did not change (data not shown).

## 684 **5 Conclusion**

685 By coupling isotope tracking techniques and a mass balance over broader spatial  
686 and temporal scales, we found that an urban river-estuarine continuum in the Chesapeake  
687 Bay, and likely similar estuaries globally can transform anthropogenic inputs of N over  
688 relatively short spatial scales. Only a small fraction of N inputs from a major wastewater  
689 treatment plant were exported out of the estuary. However, processing of N by estuaries  
690 can vary considerably across seasons and hydrologic extremes, with greater exports  
691 during periods of higher flows and cooler temperatures, and greater transformations and  
692 retention during longer hydrologic residence times and warmer temperatures. In  
693 particular, this study supports previous work, showing that non-point sources of N were  
694 more dominant during winter and spring when runoff from the watershed and estuarine  
695 flows were higher compared to summer and fall when the point-sources were more  
696 dominant, due to lower flows. These differences suggest N processing in urban estuaries  
697 would differ from those in non-urban estuaries. Also, the potential for long-term and  
698 widespread increase in water temperatures and frequency and magnitude of droughts and  
699 floods through climate change (Kaushal et al., 2010a; Kaushal et al., 2014b; Kaushal et  
700 al., 2010b), will likely influence the sources and transformation of nitrogen to the  
701 Chesapeake Bay and estuaries globally. Consequently, future efforts to manage nutrient  
702 exports along estuaries would benefit from better understanding the interactive effects of  
703 land use and climate variability on the sources, amounts, and transformations of N



704 exported to coastal waters and targeting critical times for more intensive wastewater

705 treatment.

706

#### 707 **Details on Supporting Information**

- 708 • Additional site information and details on methods
- 709 • Table with site coordinates
- 710 • Table with mixing model
- 711 • Table comparing between box model (this study) and Chesapeake Bay Model.
- 712 • A figure comparing box model results with and without bottom water isotope data

713

#### 714 **Data Availability**

715 Data used for the research in this paper is available through 4TU.centre at the following

716 DOI and URL: doi:10.4121/uuid:e68c6141-f83e-4375-ac3b-088ddf4eff51

717 <http://doi.org/10.4121/uuid:e68c6141-f83e-4375-ac3b-088ddf4eff51>

718

#### 719 **Author contribution**

720 This paper is based on work from Michael Pennino's PhD dissertation. Dr. Michael  
721 Pennino collected water samples, conducted data analysis, and wrote the manuscript. Dr.  
722 Sujay Kaushal contributed to the study design, and provided helpful feedback on data  
723 analysis and manuscript writing. Dr. Sudhir Murthy contributed to study design,  
724 provided data, and contributed to manuscript revisions. Joel Blomquist contributed to  
725 study design, sample collection, and manuscript revisions. Dr. Jeff Cornwell contributed  
726 to manuscript revisions and provided feedback on data analysis. Dr. Lora Harris



727 contributed to study design, and helped with data analysis (particularly for the box model  
728 mass balance), and manuscript writing.

729

### 730 **Acknowledgements**

731 Contact the corresponding author ([michael.pennino@gmail.com](mailto:michael.pennino@gmail.com)) regarding the nitrate  
732 isotope data. The historical water quality data used in this study was collected by the  
733 Maryland Department of Natural Resources and is available free through the Chesapeake  
734 Bay Program's Data Hub website:

735 ([www.chesapeakebay.net/data/downloads/cbp\\_water\\_quality\\_database\\_1984\\_present](http://www.chesapeakebay.net/data/downloads/cbp_water_quality_database_1984_present)).

736 This research was supported by the Washington D.C. Water and Sewer Authority. We  
737 would like to thank Sally Bowen and Matt Hall from the Maryland Department of  
738 Natural Resources (DNR) for their assistance in collecting monthly water samples along  
739 the Potomac Estuary and David Brower at the U.S. Geological Survey for help in  
740 collecting monthly river input samples for the Potomac River. We acknowledge the input  
741 provided by Lewis Linker and Ping Wang of the US EPA Chesapeake Bay Program's  
742 Modeling Team for providing simulated output from the CE QUAL ICEM model at three  
743 flux boundaries in the Potomac for comparison with our box model output. Gratitude is  
744 extended to Dr. Jeremy Testa for his suggestions regarding the box model effort. Tom  
745 Jordan also provided helpful suggestions.

746



747 **References**

- 748 Aitkenhead-Peterson, J. A., Steele, M. K., Nahar, N., and Santhy, K.: Dissolved organic  
749 carbon and nitrogen in urban and rural watersheds of south-central Texas: land use and  
750 land management influences, *Biogeochemistry*, 96, 119-129, 2009.
- 751 Betlach, M. R. and Tiedje, J. M.: Kinetic explanation for accumulation of nitrite, nitric-  
752 oxide, and nitrous-oxide during bacterial denitrification, *Applied and Environmental*  
753 *Microbiology*, 42, 1074-1084, 1981.
- 754 Boesch, D. F., Brinsfield, R. B., and Magnien, R. E.: Chesapeake Bay eutrophication:  
755 Scientific understanding, ecosystem restoration, and challenges for agriculture, *J.*  
756 *Environ. Qual.*, 30, 303-320, 2001.
- 757 Boynton, W. R., Garber, J. H., Summers, R., and Kemp, W. M.: Inputs, transformations,  
758 and transport of nitrogen and phosphorus in Chesapeake Bay and selected tributaries,  
759 *Estuaries*, 18, 285-314, 1995.
- 760 Boynton, W. R., Hagy, J. D., Cornwell, J. C., Kemp, W. M., Greene, S. M., Owens, M.  
761 S., Baker, J. E., and Larsen, R. K.: Nutrient budgets and management actions in the  
762 Patuxent River estuary, Maryland, *Estuaries Coasts*, 31, 623-651, 2008.
- 763 Buda, A. R. and DeWalle, D. R.: Dynamics of stream nitrate sources and flow pathways  
764 during stormflows on urban, forest and agricultural watersheds in central Pennsylvania,  
765 USA, *Hydrological Processes*, 23, 3292-3305, 2009.
- 766 Burns, D. A., Boyer, E. W., Elliott, E. M., and Kendall, C.: Sources and Transformations  
767 of Nitrate from Streams Draining Varying Land Uses: Evidence from Dual Isotope  
768 Analysis, *J. Environ. Qual.*, 38, 1149-1159, 2009.



769 Burns, D. A. and Kendall, C.: Analysis of delta(15)N and delta(18)O to differentiate  
770 NO(3)(-) sources in runoff at two watersheds in the Catskill Mountains of New York,  
771 Water Resources Research, 38, 2002.

772 Casciotti, K. L., Sigman, D. M., Hastings, M. G., Bohlke, J. K., and Hilkert, A.:  
773 Measurement of the oxygen isotopic composition of nitrate in seawater and freshwater  
774 using the denitrifier method, Analytical Chemistry, 74, 4905-4912, 2002.

775 Cerco, C., Kim, S. C., and Noel, M. R.: The 2010 Chesapeake Bay Eutrophication  
776 Model, A Report to the US Environmental Protection Agency and to the US Army Corps  
777 of Engineer Baltimore District. US Army Engineer Research and Development Center,  
778 Vicksburg, MD, ([http://www.chesapeakebay.net/content/publications/cbp\\_26167.pdf](http://www.chesapeakebay.net/content/publications/cbp_26167.pdf)),  
779 2010. 2010.

780 Chesapeake Bay Program: CBP Water Quality Database (1984-present),  
781 [http://www.chesapeakebay.net/data/downloads/cbp\\_water\\_quality\\_database\\_1984\\_prese](http://www.chesapeakebay.net/data/downloads/cbp_water_quality_database_1984_prese)  
782 [nt](#), Accessed August 2013, 2013. 2013.

783 Cornwell, J. C., Glibert, P. M., and Owens, M. S.: Nutrient Fluxes from Sediments in the  
784 San Francisco Bay Delta, Estuaries Coasts, 37, 1120-1133, 2014.

785 Crump, B. C. and Baross, J. A.: Particle-attached bacteria and heterotrophic plankton  
786 associated with the Columbia River estuarine turbidity maxima, Marine Ecology Progress  
787 Series, 138, 265-273, 1996.

788 Dawson, R. N. and Murphy, K. L.: Temperature dependency of biological denitrification,  
789 Water Res., 6, 71-&, 1972.



- 790 Divers, M. T., Elliott, E. M., and Bain, D. J.: Quantification of Nitrate Sources to an  
791 Urban Stream Using Dual Nitrate Isotopes, *Environ. Sci. Technol.*, 48, 10580-10587,  
792 2014.
- 793 Easterling, D. R., Meehl, G. A., Parmesan, C., Changnon, S. A., Karl, T. R., and Mearns,  
794 L. O.: Climate extremes: Observations, modeling, and impacts, *Science*, 289, 2068-2074,  
795 2000.
- 796 Elliott, A. J.: The circulation and salinity distribution of the upper Potomac estuary  
797 Maryland USA, *Chesapeake Science*, 17, 141-147, 1976.
- 798 Elliott, A. J.: Observations of meteorologically induced circulation in Potomac estuary,  
799 *Estuarine and Coastal Marine Science*, 6, 285-299, 1978.
- 800 Eyre, B. D. and Ferguson, A. J. P.: Benthic metabolism and nitrogen cycling in a  
801 subtropical east Australian Estuary (Brunswick): Temporal variability and controlling  
802 factors, *Limnology and Oceanography*, 50, 81-96, 2005.
- 803 Fawcett, S. E., Ward, B. B., Lomas, M. W., and Sigman, D. M.: Vertical decoupling of  
804 nitrate assimilation and nitrification in the Sargasso Sea, *Deep-Sea Research Part I-*  
805 *Oceanographic Research Papers*, 103, 64-72, 2015.
- 806 Filoso, S. and Palmer, M. A.: Assessing stream restoration effectiveness at reducing  
807 nitrogen export to downstream waters, *Ecological Applications*, 21, 1989-2006, 2011.
- 808 Fisher, T. R., Gustafson, A. B., Sellner, K., Lacouture, R., Haas, L. W., Wetzel, R. L.,  
809 Magnien, R., Everitt, D., Michaels, B., and Karrh, R.: Spatial and temporal variation of  
810 resource limitation in Chesapeake Bay, *Marine Biology*, 133, 763-778, 1999.
- 811 Fogel, M. and Cifuentes, L.: Isotope fractionation during primary production, Plenum  
812 Press, New York, 1993.



- 813 Gillooly, J. F., Brown, J. H., West, G. B., Savage, V. M., and Charnov, E. L.: Effects of  
814 size and temperature on metabolic rate, *Science*, 293, 2248-2251, 2001.
- 815 Granger, J., Sigman, D. M., Lehmann, M. F., and Tortell, P. D.: Nitrogen and oxygen  
816 isotope fractionation during dissimilatory nitrate reduction by denitrifying bacteria,  
817 *Limnology and Oceanography*, 53, 2533-2545, 2008.
- 818 Granger, J., Sigman, D. M., Needoba, J. A., and Harrison, P. J.: Coupled nitrogen and  
819 oxygen isotope fractionation of nitrate during assimilation by cultures of marine  
820 phytoplankton, *Limnology and Oceanography*, 49, 1763-1773, 2004.
- 821 Hagy, J. D., Sanford, L. P., and Boynton, W. R.: Estimation of net physical transport and  
822 hydraulic residence times for a coastal plain estuary using box models, *Estuaries*, 23,  
823 328-340, 2000.
- 824 Hamdan, L. J. and Jonas, R. B.: Seasonal and interannual dynamics of free-living  
825 bacterioplankton and microbially labile organic carbon along the salinity gradient of the  
826 Potomac River, *Estuaries Coasts*, 29, 40-53, 2006.
- 827 Harris, L. A. and Brush, M. J.: Bridging the gap between empirical and mechanistic  
828 models of aquatic primary production with the metabolic theory of ecology: An example  
829 from estuarine ecosystems, *Ecological Modelling*, 233, 83-89, 2012.
- 830 Hopkinson, C. S. and Vallino, J. J.: The relationships among mans activities in  
831 watersheds and estuaries - a model of runoff effects on patterns of estuarine community  
832 metabolism, *Estuaries*, 18, 598-621, 1995.
- 833 Horrigan, S. G., Montoya, J. P., Nevins, J. L., and McCarthy, J. J.: Natural isotopic  
834 composition of dissolved inorganic nitrogen in the Chesapeake Bay, *Estuarine Coastal  
835 and Shelf Science*, 30, 393-410, 1990.



836 IPCC: Climate Change 2007. The Physical Science Basis. Contribution of Working  
837 Group I to the Fourth Assessment Report of the Intergovernmental Panel on Climate  
838 Change, Cambridge University Press, Cambridge and New York, 2007.

839 Jaworski, N. A., Groffman, P. M., Keller, A. A., and Prager, J. C.: A watershed nitrogen  
840 and phosphorus balance - the upper Potomac River basin, *Estuaries*, 15, 83-95, 1992.

841 Jordan, T. E., Cornwell, J. C., Boynton, W. R., and Anderson, J. T.: Changes in  
842 phosphorus biogeochemistry along an estuarine salinity gradient: The iron conveyor belt,  
843 *Limnology and Oceanography*, 53, 172-184, 2008.

844 Jordan, T. E., Weller, D. E., and Correll, D. L.: Sources of nutrient inputs to the Patuxent  
845 River estuary, *Estuaries*, 26, 226-243, 2003.

846 Karrh, R., Romano, W., Garrison, S., Michael, B., Hall, M., Coyne, K., Reynolds, D., and  
847 Ebersole, B.: Maryland Tributary Strategy Upper Potomac River Basin Summary Report  
848 for 1985-2005 Data. Maryland Department of Natural Resources, 2007a.

849 Karrh, R., Romano, W., Raves-Golden, R., Tango, P., Garrison, S., Michael, B., Baldizar,  
850 J., Trumbauer, C., Hall, M., Cole, B., Aadland, C., Trice, M., Coyne, K., Reynolds, D.,  
851 Ebersole, B., and Karrh, L.: Maryland Tributary Strategy Lower Potomac River Basin  
852 Summary Report for 1985-2005 Data. Maryland Department of Natural Resources,  
853 2007b.

854 Karsh, K. L., Granger, J., Kritee, K., and Sigman, D. M.: Eukaryotic Assimilatory Nitrate  
855 Reductase Fractionates N and O Isotopes with a Ratio near Unity, *Environ. Sci. Technol.*,  
856 46, 5727-5735, 2012.



- 857 Karsh, K. L., Trull, T. W., Sigman, D. M., Thompson, P. A., and Granger, J.: The  
858 contributions of nitrate uptake and efflux to isotope fractionation during algal nitrate  
859 assimilation, *Geochimica Et Cosmochimica Acta*, 132, 391-412, 2014.
- 860 Kaushal, S. S. and Belt, K. T.: The urban watershed continuum: evolving spatial and  
861 temporal dimensions, *Urban Ecosystems*, 15, 409-435, 2012.
- 862 Kaushal, S. S., Delaney-Newcomb, K., Findlay, S. E. G., Newcomer, T. A., Duan, S.,  
863 Pennino, M. J., Sviririchi, G. M., Sides-Raley, A. M., Walbridge, M. R., and Belt, K. T.:  
864 Longitudinal patterns in carbon and nitrogen fluxes and stream metabolism along an  
865 urban watershed continuum, *Biogeochemistry*, DOI 10.1007/s10533-014-9979-9, 2014a.
- 866 Kaushal, S. S., Groffman, P. M., Band, L. E., Elliott, E. M., Shields, C. A., and Kendall,  
867 C.: Tracking Nonpoint Source Nitrogen Pollution in Human-Impacted Watersheds,  
868 *Environ. Sci. Technol.*, 45, 8225-8232, 2011.
- 869 Kaushal, S. S., Likens, G. E., Jaworski, N. A., Pace, M. L., Sides, A. M., Seekell, D.,  
870 Belt, K. T., Secor, D. H., and Wingate, R. L.: Rising stream and river temperatures in the  
871 United States, *Frontiers in Ecology and the Environment*, 8, 461-466, 2010a.
- 872 Kaushal, S. S., Mayer, P. M., Vidon, P. G., Smith, R. M., Pennino, M. J., Duan, S.,  
873 Newcomer, T. A., Welty, C., and Belt, K. T.: Land use and climate variability amplify  
874 carbon, nutrient, and contaminant pulses: a review with management implications,  
875 *Journal of the American Water Resources Association*, **50**, 585-614, 2014b.
- 876 Kaushal, S. S., McDowell, W. H., and Wollheim, W. M.: Tracking evolution of urban  
877 biogeochemical cycles: past, present, and future, *Biogeochemistry*, 121, 1-21, 2014c.
- 878 Kaushal, S. S., Pace, M. L., Groffman, P. M., Band, L. E., Belt, K. T., Mayer, P. M., and  
879 Welty, C.: Land use and climate variability amplify contaminant pulses, *EOS*, 91, 2010b.



- 880 Kemp, W. M., Sampou, P., Caffrey, J., Mayer, M., Henriksen, K., and Boynton, W. R.:  
881 Ammonium recycling versus denitrification in Chesapeake Bay sediments, *Limnology*  
882 and *Oceanography*, 35, 1545-1563, 1990.
- 883 Kendall, C., Elliott, E. M., and Wankel, S. D.: Tracing anthropogenic inputs of nitrogen  
884 to ecosystems, *Stable Isotopes in Ecology and Environmental Science*, 2nd Edition, doi:  
885 10.1002/9780470691854.ch12, 2007. 375-449, 2007.
- 886 Lehmann, M. F., Reichert, P., Bernasconi, S. M., Barbieri, A., and McKenzie, J. A.:  
887 Modelling nitrogen and oxygen isotope fractionation during denitrification in a lacustrine  
888 redox-transition zone, *Geochimica Et Cosmochimica Acta*, 67, 2529-2542, 2003.
- 889 Marconi, D., Weigand, M. A., Rafter, P. A., McIlvin, M. R., Forbes, M., Casciotti, K. L.,  
890 and Sigman, D. M.: Nitrate isotope distributions on the US GEOTRACES North Atlantic  
891 cross-basin section: Signals of polar nitrate sources and low latitude nitrogen cycling,  
892 *Marine Chemistry*, 177, 143-156, 2015.
- 893 Mariotti, A., Germon, J. C., Hubert, P., Kaiser, P., Letolle, R., Tardieux, A., and  
894 Tardieux, P.: Experimental-determination of nitrogen kinetic isotope fractionation - some  
895 principles - illustration for the denitrification and nitrification processes, *Plant and Soil*,  
896 62, 413-430, 1981.
- 897 Mayer, B., Bollwerk, S. M., Mansfeldt, T., Hutter, B., and Veizer, J.: The oxygen isotope  
898 composition of nitrate generated by nitrification in acid forest floors, *Geochimica Et*  
899 *Cosmochimica Acta*, 65, 2743-2756, 2001.
- 900 Mayer, B., Boyer, E. W., Goodale, C., Jaworski, N. A., Van Breemen, N., Howarth, R.  
901 W., Seitzinger, S., Billen, G., Lajtha, L. J., Nosal, M., and Paustian, K.: Sources of nitrate



902 in rivers draining sixteen watersheds in the northeastern US: Isotopic constraints,  
903 Biogeochemistry, 57, 171-197, 2002.

904 Middelburg, J. J. and Nieuwenhuize, J.: Nitrogen isotope tracing of dissolved inorganic  
905 nitrogen behaviour in tidal estuaries, Estuarine Coastal and Shelf Science, 53, 385-391,  
906 2001.

907 Middelburg, J. J. and Nieuwenhuize, J.: Nitrogen uptake by heterotrophic bacteria and  
908 phytoplankton in the nitrate-rich Thames estuary, Marine Ecology Progress Series, 203,  
909 13-21, 2000.

910 Milliman, J. D., Shen, H. T., Yang, Z. S., and Meade, R. H.: Transport and deposition of  
911 river sediment in the changjiang estuary and adjacent continental-shelf, Continental Shelf  
912 Research, 4, 37-45, 1985.

913 Nixon, S. W., Ammerman, J. W., Atkinson, L. P., Berounsky, V. M., Billen, G.,  
914 Boicourt, W. C., Boynton, W. R., Church, T. M., Ditoro, D. M., Elmgren, R., Garber, J.  
915 H., Giblin, A. E., Jahnke, R. A., Owens, N. J. P., Pilson, M. E. Q., and Seitzinger, S. P.:  
916 The fate of nitrogen and phosphorus at the land sea margin of the North Atlantic Ocean,  
917 Biogeochemistry, 35, 141-180, 1996.

918 Nowicki, B. L.: The effect of temperature, oxygen, salinity, and nutrient enrichment on  
919 estuarine denitrification rates measured with a modified nitrogen gas flux technique,  
920 Estuarine Coastal and Shelf Science, 38, 137-156, 1994.

921 Oczkowski, A., Nixon, S., Henry, K., DiMilla, P., Pilson, M., Granger, S., Buckley, B.,  
922 Thornber, C., McKinney, R., and Chaves, J.: Distribution and trophic importance of  
923 anthropogenic nitrogen in Narragansett Bay: An assessment using stable isotopes,  
924 Estuaries Coasts, 31, 53-69, 2008.



- 925 Officer, C. B.: Box models revisited. In: Estuarine and wetland processes, with emphasis  
926 on modeling, Hamilton, P. and Macdonald, K. B. (Eds.), Plenum Press, New York and  
927 London, 1980.
- 928 Paerl, H. W., Valdes, L. M., Piehler, M. F., and Stow, C. A.: Assessing the effects of  
929 nutrient management in an estuary experiencing climatic change: The Neuse River  
930 Estuary, North Carolina, *Environ. Manage.*, 37, 422-436, 2006.
- 931 Parnell, A. C., Inger, R., Bearhop, S., and Jackson, A. L.: Source Partitioning Using  
932 Stable Isotopes: Coping with Too Much Variation, *Plos One*, 5, 2010.
- 933 Parnell, A. C., Phillips, D. L., Bearhop, S., Semmens, B. X., Ward, E. J., Moore, J. W.,  
934 Jackson, A. L., Grey, J., Kelly, D. J., and Inger, R.: Bayesian stable isotope mixing  
935 models, *Environmetrics*, 24, 387-399, 2013.
- 936 Petrone, K. C.: Catchment export of carbon, nitrogen, and phosphorus across an agro-  
937 urban land use gradient, Swan-Canning River system, southwestern Australia, *Journal of*  
938 *Geophysical Research-Biogeosciences*, G01016 2010.
- 939 Pfenning, K. S. and McMahon, P. B.: Effect of nitrate, organic carbon, and temperature  
940 on potential denitrification rates in nitrate-rich riverbed sediments, *Journal of Hydrology*,  
941 187, 283-295, 1997.
- 942 Pritchard, D. W.: The dynamic structure of a coastal plain estuary, *Journal of Marine*  
943 *Research*, 15, 33-42, 1956.
- 944 R Development Core Team: <http://www.R-project.org>, 2013.
- 945 Rafter, P. A., DiFiore, P. J., and Sigman, D. M.: Coupled nitrate nitrogen and oxygen  
946 isotopes and organic matter remineralization in the Southern and Pacific Oceans, *Journal*  
947 *of Geophysical Research-Oceans*, 118, 4781-4794, 2013.



- 948 Sanford, L. P., Suttles, S. E., and Halka, J. P.: Reconsidering the physics of the  
949 Chesapeake Bay estuarine turbidity maximum, *Estuaries*, 24, 655-669, 2001.
- 950 Saunders, M. A. and Lea, A. S.: Large contribution of sea surface warming to recent  
951 increase in Atlantic hurricane activity, *Nature*, 451, 557-U553, 2008.
- 952 Sigman, D. M., Casciotti, K. L., Andreani, M., Barford, C., Galanter, M., and Bohlke, J.  
953 K.: A bacterial method for the nitrogen isotopic analysis of nitrate in seawater and  
954 freshwater, *Analytical Chemistry*, 73, 4145-4153, 2001.
- 955 Smart, S. M., Fawcett, S. E., Thomalla, S. J., Weigand, M. A., Reason, C. J. C., and  
956 Sigman, D. M.: Isotopic evidence for nitrification in the Antarctic winter mixed layer,  
957 *Global Biogeochemical Cycles*, 29, 427-445, 2015.
- 958 Testa, J. M., Kemp, W. M., Boynton, W. R., and Hagy, J. D.: Long-Term Changes in  
959 Water Quality and Productivity in the Patuxent River Estuary: 1985 to 2003, *Estuaries  
960 Coasts*, 31, 1021-1037, 2008.
- 961 US-EPA: <http://cfpub.epa.gov/npdes/cwa.cfm>, 1972.
- 962 US-EPA: <http://cfpub.epa.gov/npdes/>, 2009.
- 963 US-EPA: U.S. Environmental Protection Agency. National Pollutant Discharge  
964 Elimination System (NPDES) Stormwater Program, 2011. 2011.
- 965 USGS: US Geological Survey Surface Water Data.  
966 <http://waterdata.usgs.gov/md/nwis/uv?01646500>. Accessed June 2014, 2014. 2014.
- 967 Vavilin, V. A.: Describing a Kinetic Effect of Fractionation of Stable Nitrogen Isotopes  
968 in Nitrification Process, *Water Resources*, 41, 325-329, 2014.
- 969 Vavilin, V. A., Rytov, S. V., and Lokshina, L. Y.: Non-linear dynamics of nitrogen  
970 isotopic signature based on biological kinetic model of uptake and assimilation of



971 ammonium, nitrate and urea by a marine diatom, *Ecological Modelling*, 279, 45-53,  
972 2014.

973 Vitousek, P. M., Aber, J. D., Howarth, R. W., Likens, G. E., Matson, P. A., Schindler, D.  
974 W., Schlesinger, W. H., and Tilman, D.: Human alteration of the global nitrogen cycle:  
975 Sources and consequences, *Ecological Applications*, 7, 737-750, 1997.

976 Wang, S. Q., Tang, C. Y., Song, X. F., Yuan, R. Q., Wang, Q. X., and Zhang, Y. H.:  
977 Using major ions and delta N-15-NO<sub>3</sub><sup>-</sup> to identify nitrate sources and fate in an alluvial  
978 aquifer of the Baiyangdian lake watershed, North China Plain, *Environmental Science-*  
979 *Processes & Impacts*, 15, 1430-1443, 2013.

980 Wankel, S. D., Kendall, C., Francis, C. A., and Paytan, A.: Nitrogen sources and cycling  
981 in the San Francisco Bay Estuary: A nitrate dual isotopic composition approach,  
982 *Limnology and Oceanography*, 51, 1654-1664, 2006.

983 Waser, N. A., Yin, K. D., Yu, Z. M., Tada, K., Harrison, P. J., Turpin, D. H., and Calvert,  
984 S. E.: Nitrogen isotope fractionation during nitrate, ammonium and urea uptake by  
985 marine diatoms and coccolithophores under various conditions of N availability, *Marine*  
986 *Ecology Progress Series*, 169, 29-41, 1998a.

987 Waser, N. A. D., Harrison, P. J., Nielsen, B., Calvert, S. E., and Turpin, D. H.: Nitrogen  
988 isotope fractionation during the uptake and assimilation of nitrate, nitrite, ammonium,  
989 and urea by a marine diatom, *Limnology and Oceanography*, 43, 215-224, 1998b.

990 Wiegert, R. G. and Penaslado, E.: Nitrogen-pulsed systems on the coast of northwest  
991 Spain, *Estuaries*, 18, 622-635, 1995.



992 Xue, D. M., De Baets, B., Van Cleemput, O., Hennessy, C., Berglund, M., and Boeckx,

993 P.: Use of a Bayesian isotope mixing model to estimate proportional contributions of

994 multiple nitrate sources in surface water, Environ. Pollut., 161, 43-49, 2012.

995 Yang, Y. Y. and Toor, G. S.: delta N-15 and delta O-18 Reveal the Sources of Nitrate-

996 Nitrogen in Urban Residential Stormwater Runoff, Environ. Sci. Technol., 50, 2881-

997 2889, 2016.

998

999

1000

1001

1002

1003

1004

1005

1006

1007

1008

1009

1010

1011

1012



1013 Table 1. Seasonal comparison of N and C inputs, exports, and losses along the Potomac River Estuary.

	Nutrient	Total Inputs (kg/day)	% of Inputs from Blue Plains*	Net Export (kg/day)	% of Blue Plains Inputs Exported	Net Loss in Load along Estuary, Box 1 to 6 (kg/day)	% Net Loss in Load along Estuary, Box 1 to 6	Net Loss in Load along Estuary, Box 1 to 5 (kg/day)	% Net Loss in Load along Estuary, Box 1 to 5	Net Loads from Bay to Estuary (kg/day)
Winter	TN	49150 ± 30323	10 ± 13	19844 ± 13728	3.7 ± NA	27369 ±		16426 ±		
Spring	TN	135317 ± 14614	8 ± 0.8	68431 ± 48060	71 ± 20	49672 ± 52116	54 ± 40	29515 ± 32908	26 ± 21	473 ± 414
Summer	TN	13888 ± 596	38 ± 3	4853 ± 8326	19 ± 11	7155 ± 8370	75 ± 75	5739 ± 1832	44 ± 21	-127 ± 480
Fall	TN	15334 ± 3700	47 ± 13	-1613 ± 12124	18 ± 10	15364 ± 12548	112 ± 95	4140 ± 6607	30 ± 43	380 ± 164
Winter	NO <sub>3</sub> <sup>-</sup>	37749 ± 23574	5.7 ± 4.6	2080 ± 6235	3 ± NA	31791 ± 7417	93 ± 29	26299 ± 10069	74 ± 33	264 ± 290
Spring	NO <sub>3</sub> <sup>-</sup>	95395 ± 10416	7.4 ± 0.6	161747 ± 30039 ±	52 ± 70	40206 ± 161977	60 ± 187	30998 ± 26791	46 ± 34	32 ± 58
Summer	NO <sub>3</sub> <sup>-</sup>	7066 ± 364	49 ± 6.3	105 ± 4130	17 ± 2	5166 ± 4143	96 ± 141	4223 ± 763	77 ± 19	8 ± 109
Fall	NO <sub>3</sub> <sup>-</sup>	10526 ± 3006	53 ± 18.2	-204 ± 6278	13 ± 35	7291 ± 6812	108 ± 181	5637 ± 6817	85 ± 122	11 ± 10
Winter	δ <sup>15</sup> N-NO <sub>3</sub> <sup>-</sup>	130 ± 10	4 ± 0.4	4 ± NA	2.7 ± NA	130 ± NA	97 ± NA	77 ± NA	68 ± NA	13 ± 35
Spring	δ <sup>15</sup> N-NO <sub>3</sub> <sup>-</sup>	374 ± 3	7 ± 0.1	170 ± 547	52 ± 136	88 ± 547	48 ± 136	42 ± 71	26 ± 31	86 ± NA
Summer	δ <sup>15</sup> N-NO <sub>3</sub> <sup>-</sup>	30 ± 1	53 ± 1.6	5 ± 1	17 ± 3	27 ± 1	83 ± 3	18 ± 1	83 ± 3	-412 ± 1471
Fall	δ <sup>15</sup> N-NO <sub>3</sub> <sup>-</sup>	40 ± 5	55 ± 5.8	7 ± 8	13 ± 68	26 ± 8	87 ± 105	26 ± 13	87 ± 105	NA

1014 TN = Total Nitrogen. NA – indicates there was only one month with data for that season and thus no S.E. value.

1015 \*Blue Plains is a wastewater treatment plant.



1016 Table 2. Comparison of mean seasonal discharge and residence time within the Potomac  
1017 River Estuary

	Mean Discharge (m <sup>3</sup> /s)	Mean Residence time (days)
Winter	187 ± 60	26 ± 18
Spring	545 ± 214	57 ± 36
Summer	81 ± 29	129 ± 85
Fall	81 ± 27	196 ± 102

1018 Data is based on discharge and box model results for the period from April 2010 to  
1019 March 2011.

1020

1021

1022

1023

1024

1025

1026

1027

1028

1029

1030

1031

1032

1033

1034

1035

1036

1037



## 1038 Figures

1039 Figure 1. Map showing the Potomac River sampling stations (black diamond) and the  
1040 location of the Blue Plains Wastewater Treatment plant (WWTP, black X) just south of  
1041 Washington D.C., within the Chesapeake Bay watershed. The larger figure shows the  
1042 location of monthly extensive synoptic surveys sites and the smaller figure on upper left  
1043 shows the locations of the shorter intensive synoptic surveys. The larger figure also  
1044 shows the location for the historical Maryland DNR surface water sampling sites.

1045

1046 Figure 2. Plot of the Potomac Estuary depth with distance down-estuary showing the  
1047 location of the 6 boxes used in the box model calculations.

1048

1049 Figure 3. Longitudinal patterns in Potomac River Estuary: (a) mean annual dissolved  
1050 inorganic nitrogen (DIN) and total organic nitrogen (TON) spanning 1997 to 2005, (b)  
1051 mean seasonal DIN before year 2000 (1994 to 1999), and post 2000 (2001 to 2012), and  
1052 (c) mean (1994 to 2012) seasonal molar N:P ratio ( $\text{DIN}/\text{PO}_4^{3-}$ ), with salinity averaged  
1053 from all seasons (1984 to 2008). Note: errors bars are provided, but S.E. is relatively  
1054 small compared to concentrations. This data was obtained from the Maryland DNR and  
1055 the Chesapeake Bay Program Data Hub.

1056

1057 Figure 4. Comparison of  $\text{NO}_3^-$  vs. dissolved organic carbon (DOC). N and C data was  
1058 obtained from the Maryland DNR and the Chesapeake Bay Program Data Hub for this  
1059 study period.

1060

1061 Figure 5. Trends in (a)  $\delta^{15}\text{N}-\text{NO}_3^-$ , (b)  $\delta^{18}\text{O}-\text{NO}_3^-$ , and (c) percent contribution of nitrate  
1062 from wastewater, the atmospheric, and nitrification, based on isotope mixing model, with  
1063 distance down-estuary from wastewater treatment plant input. Error bars are standard  
1064 errors of the mean.  $N = 1$  for winter,  $N = 3$  for spring and fall, and  $N = 2$  for summer.

1065

1066 Figure 6. (a) Plot of  $\delta^{15}\text{N}-\text{NO}_3^-$  vs.  $\delta^{18}\text{O}-\text{NO}_3^-$  of nitrate from effluent water samples and  
1067 Potomac River Estuary samples, showing samples from different locations along the  
1068 estuary; the grey arrow indicates the 2:1 relationship characteristic for denitrification; and  
1069 (b) Same plot as (a), but seasonally and without the effluent or wastewater outfall values.  
1070 Not included in these plots is the box indicating the region where atmospheric nitrate  
1071 samples generally lie, from -10 to +15 for  $\delta^{15}\text{N}-\text{NO}_3^-$  and from 60 to 100 for  $\delta^{18}\text{O}-\text{NO}_3^-$ .

1072

1073 Figure 7. Comparison of salinity vs. (a)  $\text{NO}_3^-$ , (b)  $\delta^{15}\text{N}-\text{NO}_3^-$  and (c)  $\delta^{18}\text{O}-\text{NO}_3^-$ . Mixing  
1074 lines connect the mean  $\text{NO}_3^-$  concentration or isotope values at the lowest and highest  
1075 salinity values. Error bars are standard errors of the mean. For panel (a),  $N = 3$  for all  
1076 seasons, for panels (b) and (c),  $N = 1$  for winter,  $N = 3$  for spring and fall, and  $N = 2$  for  
1077 summer. Mixing line equations for  $\text{NO}_3^-$  concentrations and isotopes were obtained from  
1078 Middelburg and Nieuwenhuize (2001).  $\text{NO}_3^-$  data was obtained from the Maryland DNR  
1079 and the Chesapeake Bay Program Data Hub, covering spring 2010 to spring 2011, the  
1080 same dates as the  $\text{NO}_3^-$  isotope data.

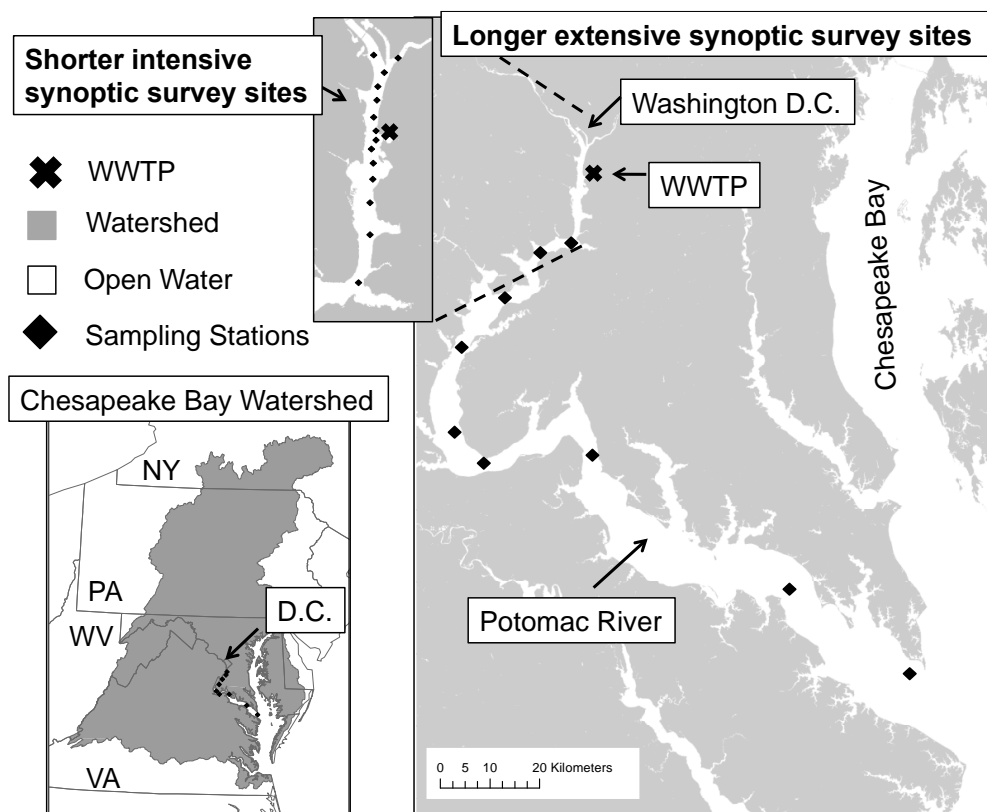
1081



1082 Figure 8. Comparing the TN fluxes along the Potomac River Estuary estimated from the  
1083 Box Model used in this study and from the results from the Chesapeake Bay nutrient  
1084 model.  
1085  
1086 Figure 9. Correlation between the fluxes estimated from the Box Model used in this study  
1087 and the Chesapeake Bay nutrient model.  
1088  
1089 Figure 10. Seasonal Box Model results showing how (a) TN, (b)  $\text{NO}_3^-$ , and (c)  $\delta^{15}\text{N-NO}_3^-$   
1090 loads vary down-estuary. Error bars are standard errors of the mean. For panels (a) and  
1091 (b),  $N = 3$  for all seasons. For panel (c),  $N = 1$  for winter,  $N = 3$  for spring and fall, and  $N$   
1092  $= 2$  for summer. TN and  $\text{NO}_3^-$  data was obtained from the Maryland DNR and the  
1093 Chesapeake Bay Program Data Hub.  
1094  
1095



1096 Figure 1.



1097  
1098

1099

1100

1101

1102

1103

1104

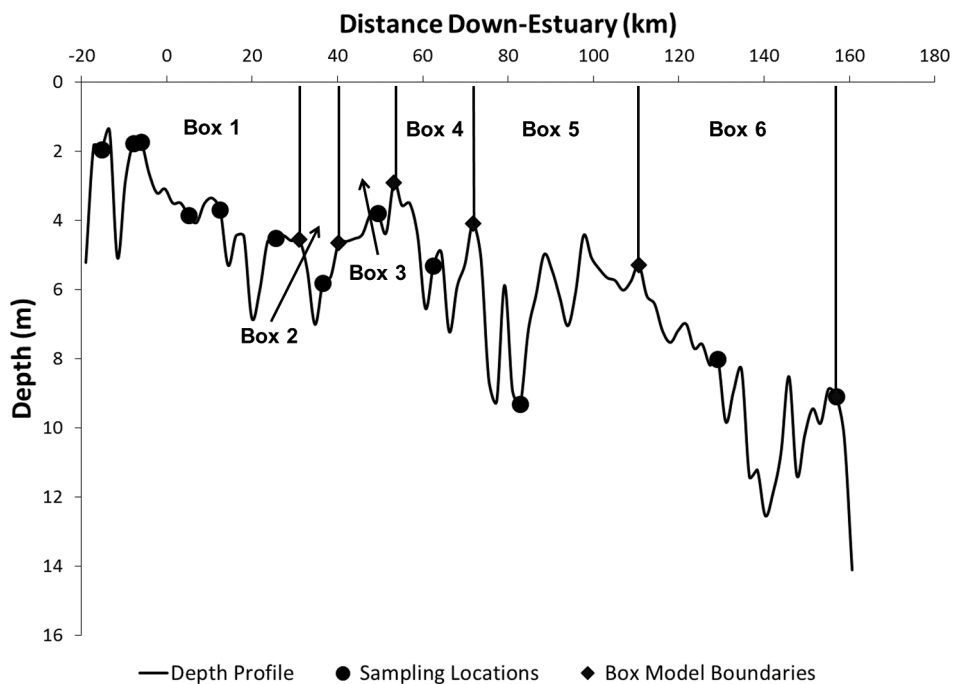
1105

1106

1107



1108 Figure 2.



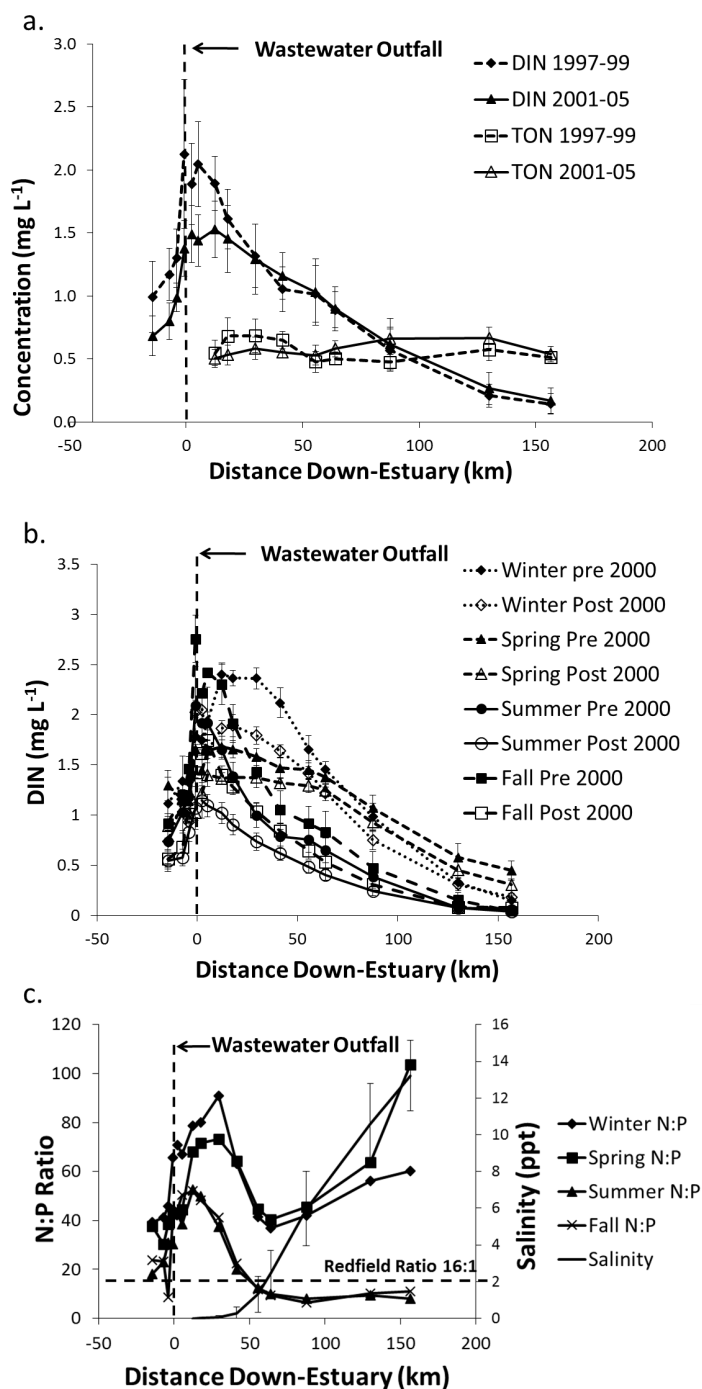
1109  
1110  
1111  
1112  
1113  
1114  
1115  
1116  
1117  
1118  
1119  
1120  
1121  
1122  
1123  
1124  
1125  
1126  
1127

1128

1129



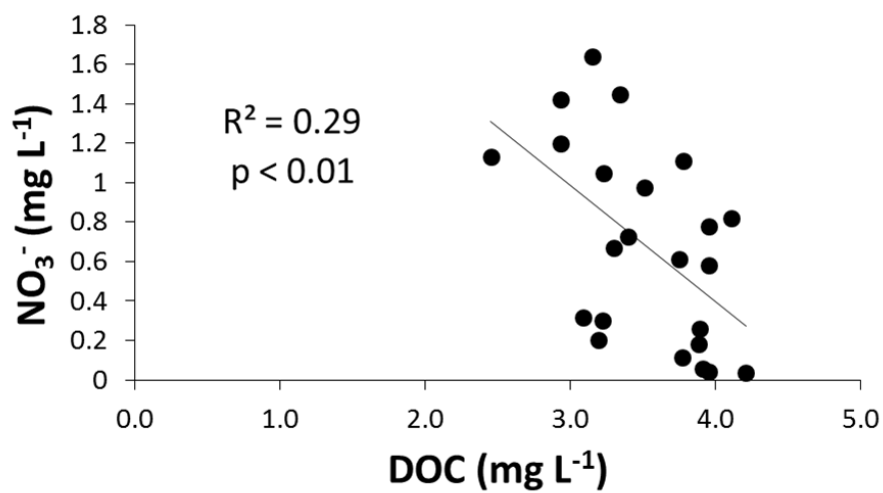
1130 Figure 3.



1131



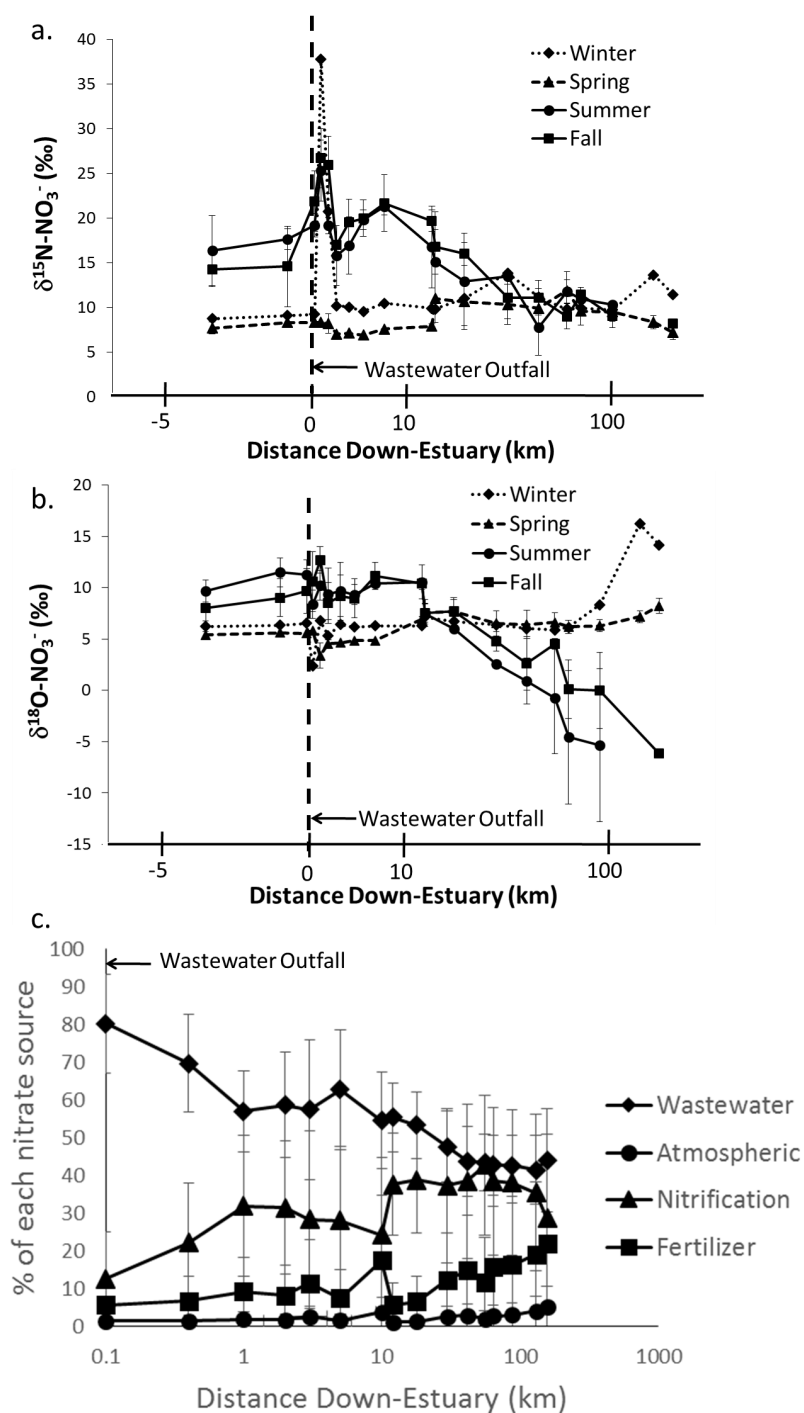
1132 Figure 4.



1133  
1134  
1135  
1136  
1137  
1138  
1139  
1140  
1141  
1142  
1143  
1144  
1145  
1146  
1147  
1148  
1149  
1150  
1151  
1152  
1153  
1154  
1155  
1156  
1157  
1158  
1159  
1160  
1161  
1162



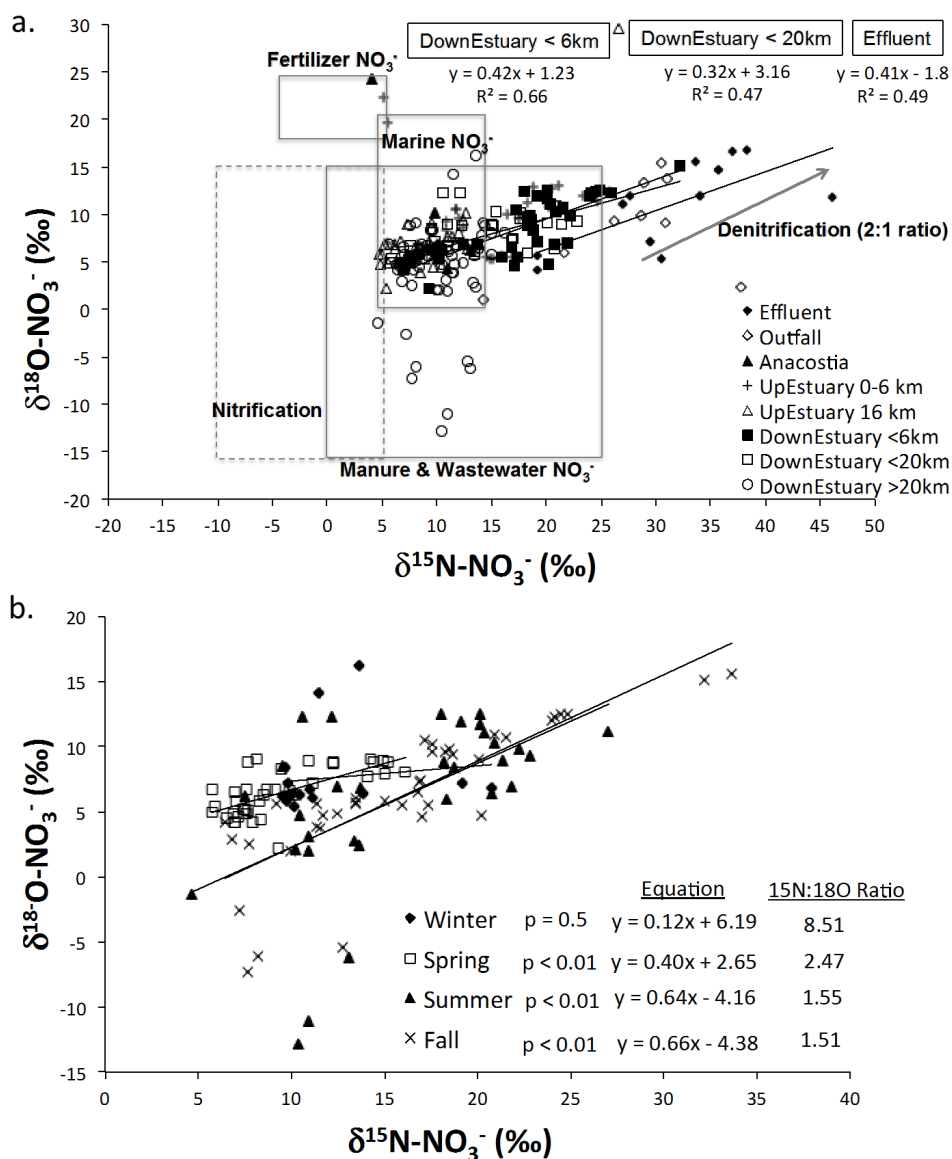
1163 Figure 5.



1164



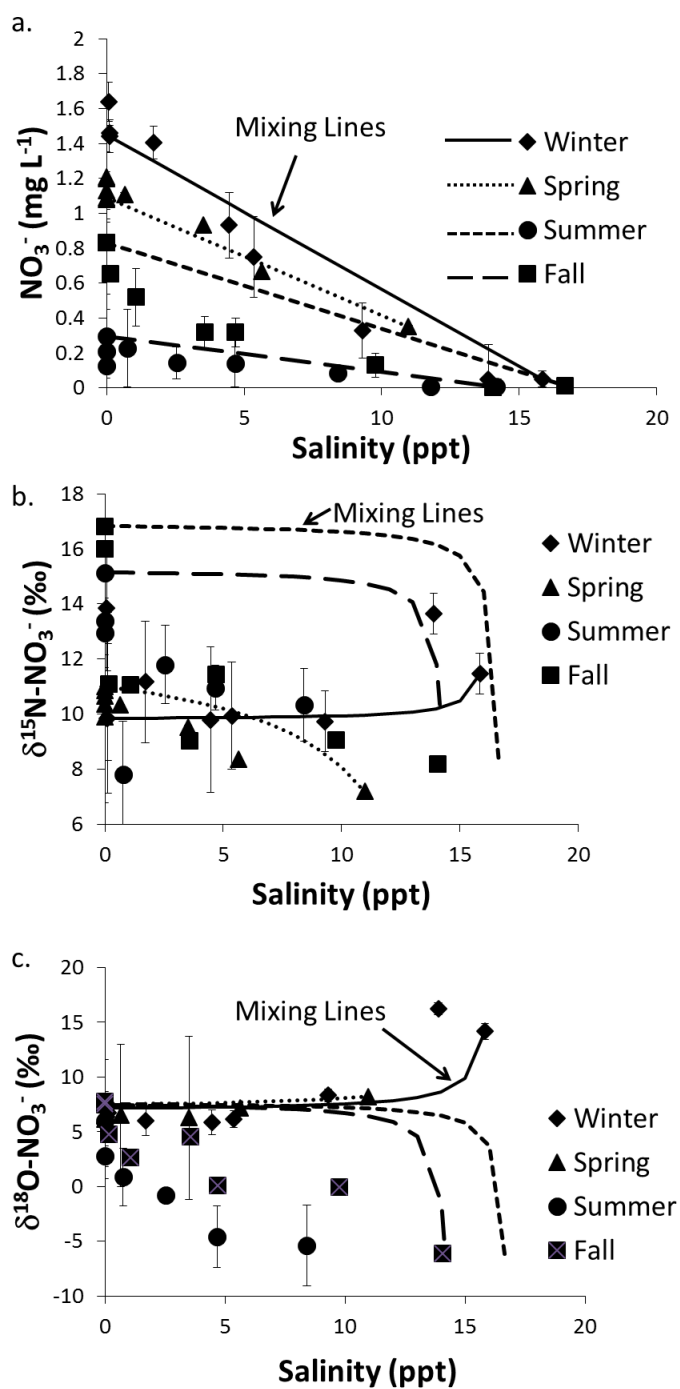
1165 Figure 6.



1166  
 1167  
 1168  
 1169  
 1170  
 1171  
 1172  
 1173  
 1174



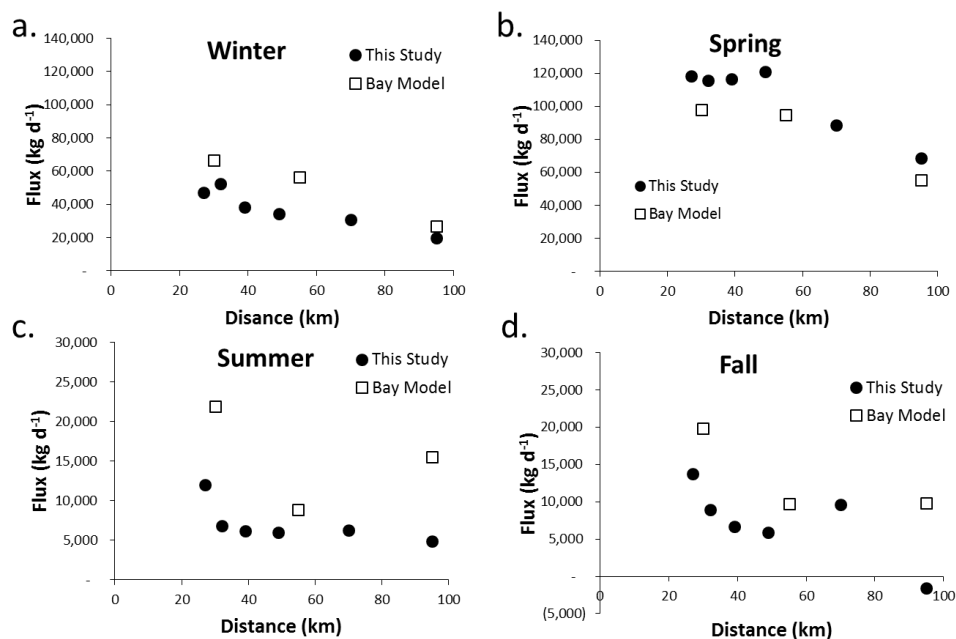
1175 Figure 7.



1176  
1177



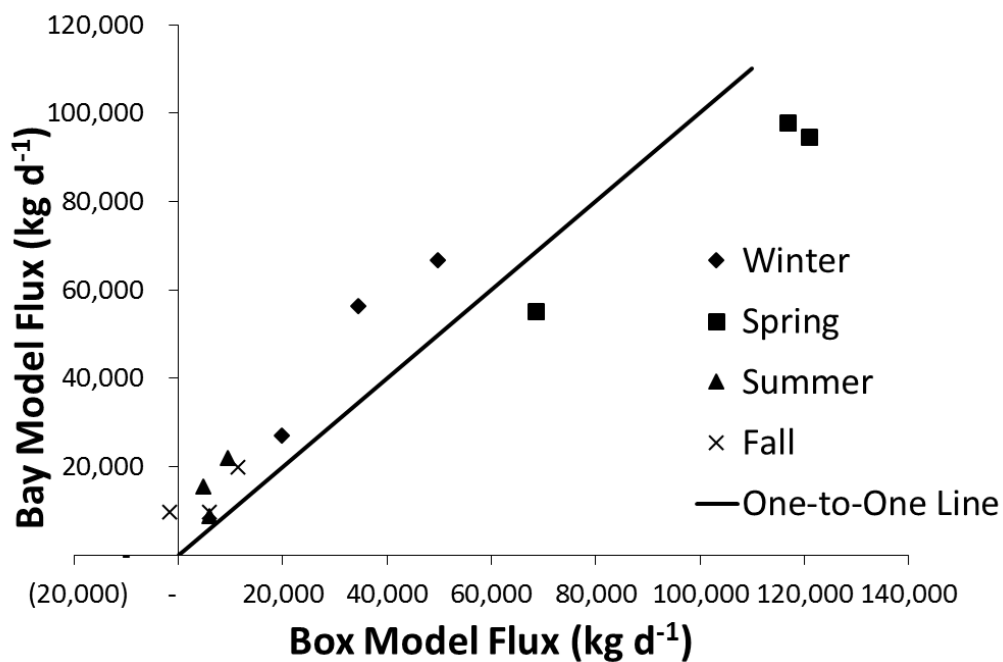
1178 Figure 8.



1179  
1180  
1181  
1182  
1183  
1184  
1185  
1186  
1187  
1188  
1189  
1190  
1191  
1192  
1193  
1194  
1195  
1196  
1197  
1198  
1199  
1200  
1201  
1202  
1203  
1204



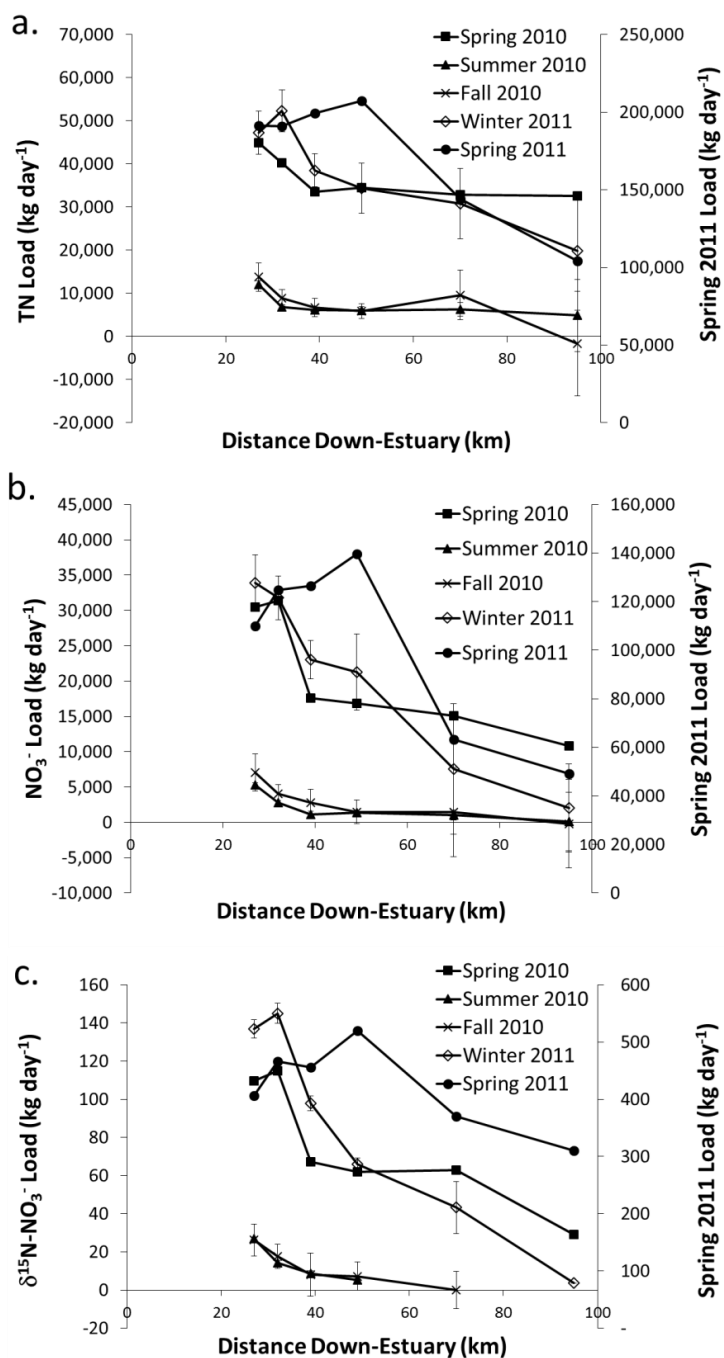
1205 Figure 9.



1206  
1207  
1208  
1209  
1210  
1211  
1212  
1213  
1214  
1215  
1216  
1217  
1218  
1219  
1220  
1221  
1222  
1223  
1224  
1225  
1226  
1227  
1228  
1229  
1230



1231 Figure 10.



1232